

The rates of Type Ia Supernovae. II. Diversity of events at low and high redshift.

Laura Greggio^{1*}

¹INAF - Osservatorio Astronomico di Padova, Vicolo dell'Osservatorio 5, I-35122 Padova

Accepted ... Received ... ; in original form ...

ABSTRACT

This paper investigates on the possible systematic difference of Supernovae Ia (SN Ia) properties related to the age and masses of the progenitors that could introduce a systematic bias between low and high redshift SN Ia's. The relation between the main features of the distribution of the delay times (DTD) and the masses of the progenitors is illustrated for the single (SD) and double degenerate (DD) models. Mixed models, which assume contributions from both the SD and DD channels, are also presented and tested versus the observed correlations between the SN Ia rates and the parent galaxy properties. It is shown that these correlations can be accounted for with both single channel and mixed models, and that the rate in S0 and E galaxies may effectively provide clues on the contribution of SD progenitors to late epoch explosions. A wide range of masses for the CO WD at the start of accretion is expected in almost all galaxy types; only in galaxies of the earliest types the properties of the progenitors are expected to be more uniform. For mixed models, late type galaxies should host SD and DD explosions in comparable fractions, while in early type galaxies DD explosions should largely prevail. Events hosted by star forming galaxies span a wide range of delay times; *prompt* events could dominate only in the presence of a strong star-burst. It is concluded that nearby SN Ia samples should well include the young, massive and hot progenitors that necessarily dominate at high redshift.

Key words: stars: evolution – supernovae: general – galaxies: evolution – cosmology: distance scale

1 INTRODUCTION

Type Ia Supernovae (SN Ia) provide an important contribution of iron to the interstellar medium (Matteucci & Greggio 1986). Because of this, the rate of SN Ia explosions, and its secular evolution are fundamental for understanding abundances and abundance patterns in stellar systems, in galaxy clusters and in the intergalactic medium. Due to the high energy release of each event, the rate of SN Ia explosions also impacts on the evolution of gas flows in Elliptical galaxies (Ciotti et al. 1991), and on the feedback process which follows from an episode of star formation (SF). The rate of nucleosynthetic and energetic input from SN Ia's critically depend on the distribution of the delay times (DTD), the delay time being the time elapsed between the birth of the SN Ia progenitor star and its final explosion. In the current literature, the shape of the DTD is still considerably debated (see Greggio, Renzini & Daddi 2008 and references therein), partly because the SN Ia progenitor's have not been unequivocally identified.

Most notably, Type Ia Supernovae are crucial cosmological probes, e.g. having provided the first evidence for cosmic acceleration (Riess et al. 1998; Perlmutter et al. 1999). Their use in cos-

mology is subject to the *standardisation* of their light curve, i.e. the ability to relate a distance independent quantity to the absolute magnitude at maximum light. For example, the Phillips relation links the SN Ia magnitude at maximum (e.g. $M_{B,\max}$) to its dimming in the first 15 days after maximum (Δm_{15} , a measure of the decline rate) (Phillips 1993; Altavilla et al. 2004). While the relation very likely reflects different production of radioactive ^{56}Ni in the explosion (Arnett 1982; Mazzali et al. 2001), the physical mechanism which causes this diversity is not clear, nor is the reason for the observed dispersion of the relation, part of which could be of intrinsic origin. In most practical applications the *standardisation* of the SN Ia light curves involves the use of the *stretch* parameter (s , Perlmutter et al. 1999), which is related to the width of the light curve and the magnitude at maximum light, based on observational data. Therefore, at present, the *standardisation* of the SN Ia light curves is fully empirical, and based on events at low redshift: if a systematic different relation holds for high z events (either in the average value, or in the dispersion, or both) the cosmological application of SN Ia's as distance indicators would be called into question. Big, homogeneous samples of nearby events are currently being constructed, from which robust correlations can be derived, and peculiar events single out (e.g. Hicken et al. 2009), but ultimately, we want to assess whether the SN Ia light curve *stretching*

* E-mail: laura.greggio@oapd.inaf.it

works in the same way at high and low redshift. It is then foremost important to understand the diversity of SN Ia events, and to check whether this is related to parameters like age and metallicity, which both increase systematically from high to low redshift.

Several observational attempts have been performed to clarify this issue. A relation between the ^{56}Ni mass and the metallicity of the progenitor is expected on the basis of the nucleosynthetic processing (Timmes, Brown & Truran 2003); this prediction has been studied by trying to determine the metallicity of individual progenitors (e.g. Ellis et al. 2008), as well as that of the stellar population hosts (Gallagher et al. 2008; Howell et al. 2009). So far the results are not conclusive, and metallicity does not appear to be the most important parameter driving the diversity (see Howell et al. 2009 for a thorough discussion). In this respect, it is worth noting that a sizable fraction of mass in stars in the local universe belongs to populations that are both old and metal rich (Renzini 2006 and references therein); therefore also at high redshift an important fraction of SN Ia events come from high metallicity stars. Thus, unless the metallicity dependence of the SN Ia light curve is very pronounced, the trend of its properties with redshift related to the change of (average) metallicity should be weak. More significant are the empirical correlations found between the light curves and the youth of the galaxy host. Literature results include the average Δm_{15} being higher in later galaxy types (Altavilla et al. 2004); brightest events occurring preferentially (if not only) in hosts with high SF rate per unit mass (Gallagher et al. 2008); a correlation between the ^{56}Ni mass and the average age of the SN Ia host, with only faint events in galaxies with average ages older than ~ 3 Gyr (Howell et al. 2009; Neill et al. 2009). The observed trends all point in the same direction, i.e. the younger the stellar population the more energetic its SN Ia, but the details differ. For example, Gallagher et al. (2008) find that SN Ia's in galaxies with high specific SF span a narrow range in V magnitude at maximum, while the diversity is much more pronounced at low specific SF. On the other hand, Howell et al. (2009) find a wide range of ^{56}Ni mass in events hosted by young stellar populations, which suggests that diversity is a feature of star forming galaxies. Altavilla et al. (2004) find a wide range of SN Ia light curve properties in both early and late type galaxies; Neill et al. (2009) find that faint events occur only in high mass galaxies, suggestive of a uniformity of SN Ia's in old stellar populations. Likely, the picture is confused because different authors use different proxies to characterise the light curve of SN Ia's (stretch parameter, Δm_{15} , magnitude at maximum in some photometric band, ejected ^{56}Ni), and the age of the parent stellar population (light or mass averaged age, spectral indices, morphological type). The empirical route to study this issue is further complicated by the effect of extinction which is difficult to correct for in the individual events (e.g. Nobili & Goobar 2008).

From the conjectural point of view, the claim of two populations for SN Ia's (Mannucci, Della Valle & Panagia 2006), one (*prompt*) supplying events within the first 0.1 Gyr from the SF episode, and one (*tardy*) providing explosions over the whole remaining age range (but with a much lower efficiency) has suggested the existence of two distinct channels for SN Ia production, possibly characterised by different light curve parameters. Since at high redshift the SN Ia production via the *prompt* channel must prevail, a systematic evolution of the Phillips relation could be present, related to the change of mixture of *prompt* and *tardy* explosions.

From the stellar evolution point of view, while it is generally agreed that SN Ia explosions are due to the ignition of fuel in CO white dwarfs (WD), the specific path to the successful event is still debated. The lack of hydrogen lines in most SN Ia spectra has tradi-

tionally lead to exclude single stars (at the end of their evolution on the Asymptotic Giant branch) as viable candidates for SN Ia's. The explosion of a (naked) WD may be obtained via accretion from a close companion in a binary system, either as a consequence of Helium detonation, when the accreted He layer reaches a critical mass (sub-Chandrasekhar models, hereinafter Sub-Chandra), or of Carbon deflagration, when the CO WD reaches the Chandrasekhar mass (hereinafter Chandra) (see Hillebrandt & Niemeyer 2000). Different progenitor models correspond to different companions of the WD, which can be non degenerate (MS or post MS) or degenerate stars (another WD); the relative evolutionary channels are commonly known as Single (SD) and Double Degenerate (DD), respectively. Therefore, stellar evolution in a close binary system does provide two different channels for SN Ia production, and also two different kinds of explosion. In each case, though, the range of delay times can be very wide, from ~ 40 Myr (the lifetime of an $8 M_{\odot}$ star, i.e. \sim the most massive CO WD progenitor) up to a Hubble time, so that each channel can accommodate *prompt* and *tardy* events. At the same time, a systematic variation of the exploding WD parameters (e.g. the range of initial mass of the primary in successful systems) with the delay time is expected within each channel, and this could account for the observed diversity, as well as imply correlations with the age of the parent stellar population.

From the observational point of view, there is no clear indication decisively supporting one channel over the other. The circumstellar material detected for the event SN 2006X (Patat et al. 2007) has been interpreted as favouring the Single Degenerate model, while the lack of it in other events is more easily understood within the Double Degenerate model (see Simon et al. 2009). According to Kasen (2010) theoretical computations, the presence of a companion should cause an excess emission in the early light curve, which originates from the collision of the ejecta with the companion. The phenomenon, which should be detectable for $\sim 10\%$ of the SD events, has not been reported so far, and provides a very interesting test of the progenitor model. Statistics of potential progenitors for the two models is also not conclusive. On the one hand there are many types of interacting binaries containing a WD plus a non degenerate star (Parthasarathy et al. 2007), like cataclysmic binaries, symbiotic systems and the particularly promising class of Supersoft X-ray sources, but it's not clear whether the population of good candidate SN Ia precursors among them is abundant enough to account for the observed SN Ia rate (Munari & Renzini 1992; Kenyon et al. 1993; Di Stefano et al. 2009). On the other hand, the inventory of close double degenerates from the SPY project did yield one system with total mass larger than the Chandrasekhar limit and close enough to merge within a Hubble time (Napiwotzki et al. 2005), showing that potential SN Ia progenitors can be found among DDs as well. A few events have been reported to require a Super-Chandrasekhar WD mass (Howell et al. 2006; Yamanaka et al. 2009): these are more easily explained as DD mergers. Meanwhile, single degenerate systems containing a WD with mass close to the Chandrasekhar limit have been discovered, like RS Oph (Hachisu, Kato & Luna 2007) and HD 49798/RX J648.0-4418 (Mereghetti et al. 2009), which are very good candidate SN Ia precursors. These evidences may well suggest that both channels are providing SNIa events with comparable efficiency.

In this paper some general features of the DTD which are expected from stellar evolution in close binaries are illustrated, following the analytical parametrisation presented in Greggio (2005) (Paper I), and described in Sect. 2. The dependence of the DTD on the major parameters is considered next, focusing on the possibil-

ity of realising strong discontinuities which may justify the concept of *prompt* and *tardy* events. The systematic variation with the delay time of some properties of the progenitors (i.e. WD cooling times, mass of the CO WD at the start of accretion, total mass of the DD systems) is also examined. These two aspects impact on the possibility of systematic differences between low and high redshift samples of SN Ia, and are discussed in Sect. 3, separately for SD and DD models. Mixed (SD + DD) DTD models are presented in Sect. 4, where the possibility of constraining the mix from the observations is discussed. The results are summarised and discussed in Sect. 5; conclusions are drawn in Sect. 6.

2 THE ANALYTIC APPROACH TO THE DTD

The standard evolutionary scenario to SN Ia explosion starts with a close binary system in which the primary is an intermediate mass star, so that the first Roche lobe overflow (RLOf) leaves a CO WD. Low mass stars ($M \lesssim 2M_{\odot}$) do produce CO WDs, but in a close binary they can do so only if the first mass exchange takes place after the He flash. Since the stellar radii at He flash are large (hundreds of solar radii), and since the distribution of the original separations A_0 scales as $1/A_0$, in most cases low mass primaries in close binary systems will fill their Roche lobe (RL) while on the first Red Giant branch, thereby producing Helium, rather than CO, WDs. Therefore, reasonable limits to the primary mass (m_1) in SN Ia progenitor systems are 2 and $8 M_{\odot}$. When the secondary fills its RL there are two possibilities: either the CO WD accretes and burns the Hydrogen rich material remaining compact inside its RL, or a common envelope (CE) forms around the two stars. In the first case, the WD grows in mass and when conditions are met, a SN Ia explosion occurs; in the second case, due to the action of a frictional drag force, the CE is eventually expelled, while the binary system shrinks (Iben & Tutukov 1987). If the secondary is relatively massive, the outcome of the CE is a CO WD + Helium star system. Further evolution causes the He star to expand and fill its RL, pouring Helium rich material on the companion, and the CO WD has again the possibility of accreting and growing up to explosion conditions (Iben & Tutukov 1994; Wang et al. 2009). Both these paths to the SN Ia event are SD channels, but in the first one (H-rich SD channel) some H is expected in the vicinity of the SN Ia which may show up in the spectrum, while in the second one (Helium star channel) no H-rich material should be around.

If the CO WD does not accrete the donated Helium, a CE phase sets in again, leading to a close CO+CO WD system. Angular momentum losses via gravitational wave radiation will eventually lead the system to merge, and, if its total mass exceeds the Chandrasekhar limit, explosion may arise. This is the DD channel to SN Ia, as provided by intermediate mass binaries. A DD system may also be formed when the secondary is a low mass star, which fills its RL when its He core is degenerate. In this case, the CE phase leaves a close binary with one CO and one He WD, but, typically, the total mass of the DD system does not reach the Chandrasekhar limit (Yungelson 2005; Ruiter, Belczynski & Fryer 2009). Therefore this channel provides mainly sub-Chandra events; while potentially important for the SN Ia's, especially at late delay times, this path is neglected here because sub-Chandra explosions do not provide a good fit to light curves and spectra of the majority of SN Ia's (Hoefflich et al. 1996; Nugent et al. 1997; Hillebrandt & Niemeyer 2000).

Upon specifications of the distribution of the initial parameters (m_1, m_2, A_0), Binary Population Synthesis (BPS) codes compute the

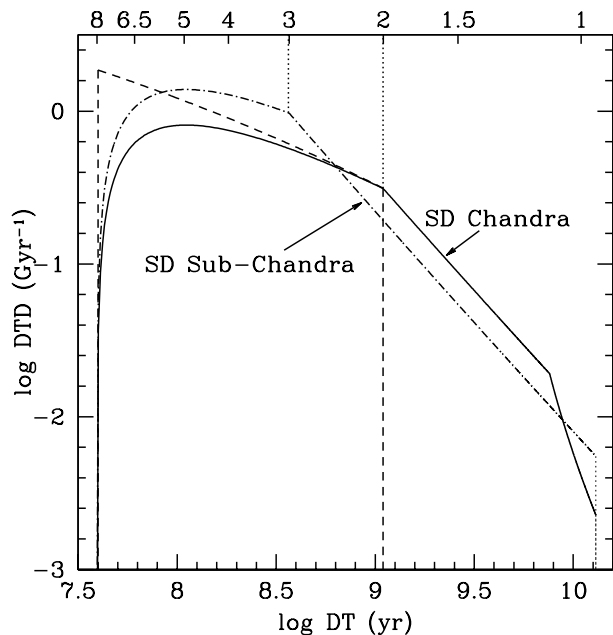


Figure 1. Distribution of the delay times for SD models, Chandra (solid) and Sub-Chandra (dot-dashed). The DTD is normalised to 1 over the range 0.04 to 13 Gyr. The upper axis is labelled with the value of the stellar mass (in M_{\odot}) evolving off the MS at the corresponding a delay time labelled on the lower axis. A Salpeter IMF for the primaries, a flat distribution of the mass ratios, and $m_1 \geq 2$ ($3 M_{\odot}$ for Chandra (Sub-Chandra) models have been adopted. The dashed line shows the trend of the CO WD formation rate from the primaries, which may represent an upper limit to the slope of the DTD for the MS+WD channel. This function, plotted on the logarithmic scale, is not normalised to 1 over the delay time range.

evolution of a population of binaries through these complicated paths, determine the partition of the population in the various channels, and the delay times of the explosions. The results are sensitive to the recipes used to follow the evolution, most notably the criteria to decide what happens when a star fills its RL. Critical prescriptions regard the occurrence of CE or not, the outcome of mass exchange, the accretion modalities on the WD, whether fuel ignition leads to accretion induced collapse or to a thermonuclear explosion (Nomoto & Iben 1985; Yoon et al. 2007; Nomoto et al. 2009; Piersanti et al. 2009). The DTD from simulations may present discontinuities due to the switch on/off of one of the channels, and/or to an abrupt variation of the efficiency with which one channel is providing SN Ia's, as a function of the original binary parameters. For example, a narrow DTD, centred on a characteristic delay time, can be produced by suppressing all but one of the channels, and narrowing the range of the progenitor masses. These (putative) discontinuities, and their location in delay time, follow from the prescriptions adopted in the BPS code. Many of the parameters which need to be specified are very poorly constrained (e.g. the efficiency α_{CE} of the CE phase which controls the degree of shrinkage of the system); therefore the specific realisations can be *up to date*, but remain uncertain.

An alternative approach to derive the DTD of SN Ia explosions consists in characterising its shape using general stellar evolution arguments, and introducing a parametrisation of a few astrophysical variables believed to play an important role. This approach was followed by Greggio & Renzini (1983) for the SD channel, improved in Greggio (1996) to accommodate Sub-Chandra explosions, and

further developed in Paper I, where analytic functions for the DTD are derived for both the SD and the DD channels. Compared to the numerical results from BPS, these functions provide a more flexible tool to investigate on the predictions from different progenitor models on various observables, thereby offering a way to constrain those astrophysical parameters which are recognised as crucial. On the other hand, in order to derive the analytic functions, some approximations and assumptions have to be made, which are summarised in the following. We refer the reader to Paper I for the detailed derivation of the analytic DTDs.

2.1 The Single Degenerate channel

Regardless the specific path, the delay time for SD channels is very close to the evolutionary lifetime of the secondary star off the MS ($\tau_n(m_2)$): for the H-rich SD explosion the extra time spent to reach the RL dimensions, and the accretion timescale during which the CO WD grows to ignition conditions are both much smaller than $\tau_n(m_2)$. For the Helium star channel, some correction (of about 10%) should be applied to account for the He burning lifetime of the former secondary; in practise however $\tau_n(m_2)$ fairly represents the total delay time also in this case. Therefore, for the SD channel there is a one to one correspondence between the mass of the secondary and the delay time, so that the distribution of the delay times is:

$$f_{\text{ia}}(\tau) \propto n(m_2) \cdot |m_2| \quad (1)$$

where $n(m_2)$ is the distribution of the secondary masses in systems which provide successful explosions through this channel, and $|m_2|$ is the rate of change of the stellar mass evolving off the main sequence. The latter factor is a robust prediction of stellar evolution theory; the first factor can be derived analytically by convolving the distribution of primary masses with the distribution of the mass ratios ($q = m_2/m_1$) in binary systems. If all SN Ia's were arising from this evolutionary path, the range spanned by m_2 should go from $\sim 8 M_\odot$ down to $\lesssim 1 M_\odot$, to account for the wide range of delay times implied by SN Ia events happening in all galaxy types (Greggio & Renzini 1983). The solid line in Fig. 1 shows the DTD for the SD Chandra channel under this hypothesis. The two cusps mark the setting in of two restrictions on the parameter space leading to explosion: the first corresponds to the minimum mass of the primary, which is set to $2 M_\odot$ since the exploding WD should be composed of CO, rather than He rich material. The later cusp is related to the requirement of totalling a Chandrasekhar mass to ensure explosion with a relatively low mass secondary: as the delay time grows long, the progressively lighter secondary ought to combine with a progressively heavier CO WD (hence heavier m_1) to meet the Chandrasekhar limit. When the lower limit on m_1 becomes larger than $2 M_\odot$ the second cusp occurs. This restriction does not apply to Sub-Chandra events (dot-dashed line); thus, in this case, the DTD presents only one cusp, motivated by the requirement of a minimum primary mass of $3 M_\odot$ as suggested by the models in Woosley & Weaver (1994).

A final remark concerns the WD + MS channel proposed by van den Heuvel et al. (1992): in this model the companion fills its RL before core H exhaustion, and the delay time could be appreciably shorter than the evolutionary lifetime of the secondary. The derivation of an analytic DTD is hardly possible in this case, since the time at which RLOf happens depends on the evolution of the binary separation as determined by several physical processes, e.g. CE evolution, magnetic braking, tidal interactions (Iben 1991). However, the primary star still has to evolve and produce a CO

WD; therefore, for a given system, the delay time will be comprised between the evolutionary lifetimes of the primary and that of the secondary. If accretion starts soon after the formation of the CO WD, the distribution of the delay times will be given by Eq.(1) with m_1 replacing m_2 , i.e. the WD formation rate from the primary. If accretion is delayed until the secondary reaches core Hydrogen exhaustion the DTD will be given by Eq.(1). The dashed line in Fig. 1 shows the CO WD formation rate (arbitrarily shifted) from primary stars with mass between 2 and $8 M_\odot$, having assumed a Salpeter IMF. We may expect that the DTD for the MS+WD channel has an intermediate slope between the dashed and the solid line, i.e. more skewed at the short delays compared to Eq.(1), but not dramatically different.

2.2 The Double Degenerate channel

The delay time for the DD systems is the sum of the MS lifetime of the secondary ($\tau_n(m_2)$, hereafter τ_n) plus the time taken by the gravitational wave radiation to get the DD system into contact (τ_{GW}). The latter time delay depends on the separation (A) and masses of the components of the DD system at birth; if both m_1 and m_2 are intermediate mass stars ($\geq 2 M_\odot$) this delay can be approximated as $\tau_{\text{GW}} = 0.6 A^4 M_{\text{DD}}^{-3}$ Gyr, where M_{DD} is the total mass of the DD system, and both A and M_{DD} are in solar units (Paper I). For what explained above, this limit on the masses of both binary components corresponds to considering CO + CO DD systems; besides, the limit $m_2 \geq 2 M_\odot$ implies a maximum delay τ_n of 1 Gyr. The delay τ_{GW} , plotted in the left panel of Fig. 2, is very sensitive to both A and M_{DD} , and in principle it ranges from virtually zero, for the most massive / closest systems, up to infinity for the least massive / widest ones. Fixed limits apply to M_{DD} , from $1.4 M_\odot$ (Chandra explosions) to $\sim 2.4 M_\odot$, when both components in the primordial system are of $8 M_\odot$ ¹. More elusive is the allowed range for A , although it must be smaller than $\sim 4 R_\odot$ in order to provide events within a Hubble time.

Typically, the separation of the DD systems at birth is the result of evolution through at least 2 RLOf episodes. Given the difficulty of describing this complex hydrodynamical phase, the results of the application of the various recipes in the literature are uncertain. In this respect, it is important to notice that a substantial shrinkage is necessary to account for SN Ia events within a Hubble time from DD systems, since the first RLOf occurs when the separation A_0 ranges from several $10 R_\odot$ (to avoid premature merging), to several $100 R_\odot$ (to get RLOf at all, see Iben & Tutukov 1987). Therefore, the prescription used in BPS codes to determine the degree of shrinkage should be accurate at a level of $\sim 1\%$ to yield correct results on an individual binary.

The sensitivity of the ratio A/A_0 to the commonly adopted literature descriptions of the CE phase is explored in Paper I. It appears that when the α_{CE} formalism (Webbink 1984) is applied to two mass exchange phases, the ratio is very small, so that only initially wide systems manage to populate the relevant range of separations (up to a few R_\odot). Conversely, if the first of the two CE phases is regulated by the Nelemans et al. (2000) (angular momentum loss) recipe, the ratio A/A_0 covers a ~ 2 orders of magnitude range, depending on the masses of the components. Moreover, in the former case, the heavier the original binary the lower the A/A_0

¹ The remnant of an $8 M_\odot$ star is assumed to be a CO WD of $1.2 M_\odot$, consistent with the empirical relation in Williams, Bolte & Koester (2004) and in Kalirai et al. 2008

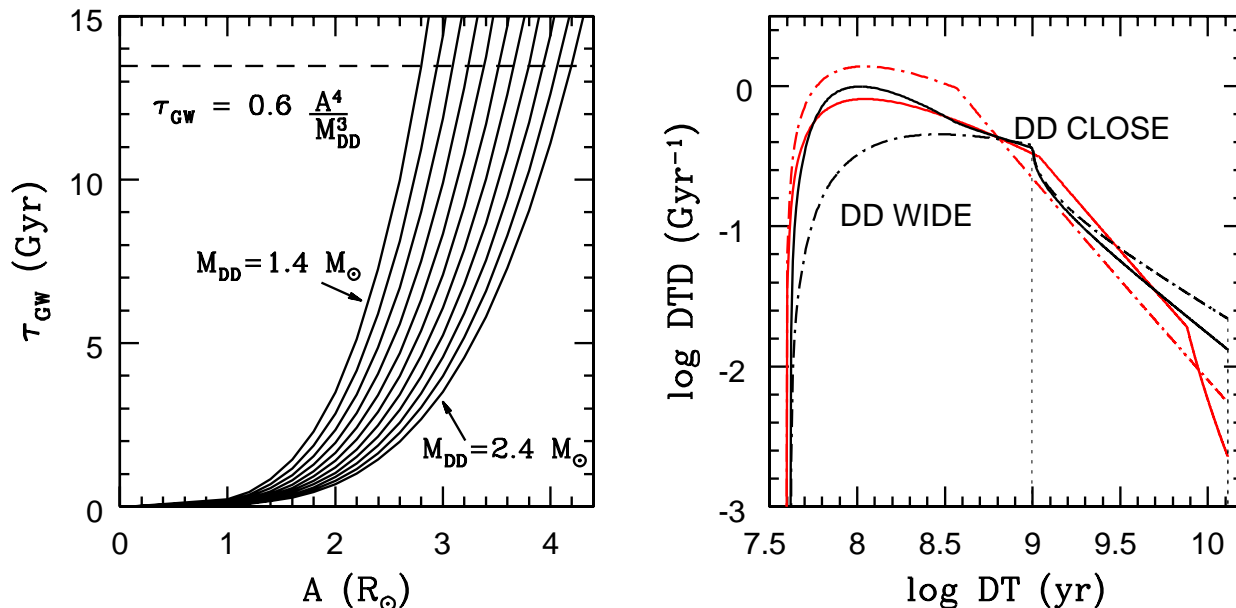


Figure 2. Left: the delay time due to the gravitational wave radiation, as given by the labelled (approximate) relation, as function of the initial separation of the DD systems, and for M_{DD} ranging from 1.4 to 2.4 M_{\odot} in steps of 0.1 M_{\odot} . Right: the distribution of the delay times for DD models, CLOSE (solid) and WIDE (dot-dashed), in the same units as in Fig. 1. Adopted parameters include a Salpeter IMF for the primaries, a flat distribution of the mass ratios, $\tau_n \leq 1$ Gyr, and flat distribution of the separations A . The DTDs for the SD models are plotted in red for comparison.

ratio: this is because in the α_{CE} formalism the shrinkage at each CE phase is proportional to the binding energy of the envelope of the donor, which is larger when the donor is more massive. Thus, the larger m_2 , the shorter τ_n and the shorter τ_{GW} : this skews the DTD towards the short delay times. When the Nelemans’ formalism is applied, instead, no strong relation appears to emerge between the initial masses of the binary components and the shrinkage, so that τ_n and τ_{GW} are likely to be uncorrelated, as well as M_{DD} and A .

On this premises, analytic distributions of the delay times for the DD channel have been derived in Paper I in two flavours: the DD-CLOSE model, in which at each m_2 the delay time varies between a minimum ($=\tau_n(m_2)$) and a maximum delay, whose value increases as m_2 decreases. In this scenario, a wide portion of the initial parameter space (m_1, m_2, A_0) maps into short delay times, while the long delay times are populated with only the less massive binaries. The DD-WIDE model, instead, assumes that A and M_{DD} are independent variables, and their distributions concur to shape the distribution of the gravitational wave radiation delay. The variables τ_n and τ_{GW} are also assumed to be basically independent, except for a correlation between m_2 (i.e. τ_n) and M_{DD} , to account for the fact that the heavier the original secondary, the more massive the DD remnant. As a result, in the DD-WIDE channel the upper limit to τ_{GW} is greater than the Hubble time irrespective of the mass of the original binary, and the population at long delay times of the corresponding DTD is enhanced. Simple power laws are assumed to describe the distribution of τ_{GW} (CLOSE DDs) and A (WIDE DDs), with parametrised exponents respectively called β_g and β_a . The shape of the distribution of M_{DD} is found to be relatively unimportant.

Admittedly, the above approximations and the assumptions are rough and do not punctually describe the outcome of the evolution of close binaries, SN Ia progenitors. However, the range

spanned by M_{DD} and A for events within a Hubble time are small, so that the assumption of smooth distributions of these parameters is likely appropriate. The main features of the curves are determined by the gravitational wave radiation clock, which implies that the distribution of τ_{GW} is skewed at the short end, unless all successful DDs are born very wide. This characteristic can be judged by projecting a flat distribution of A into the corresponding distribution on τ_{GW} in Fig. 2, left panel.

The right panel of Fig. 2 shows the DTD for CLOSE DDs and WIDE DDs, normalised to 1 over the range of delay times up to 13 Gyr. The distributions can be viewed as a modification of the SD case, where systems with given τ_n populate a range of delay times longer than this due to the extra delay τ_{GW} . The WIDE DD case is the least populated at the short delay times, the CLOSE DD the most, since in this case the great majority of systems have a short τ_{GW} . Notice that delay times in excess of 1 Gyr are populated only with systems whose τ_{GW} is longer than some limit, since by construction a maximum τ_n of 1 Gyr is imposed. This is the reason for the presence of the cusp in the DTDs: at this delay time a fixed limit on the allowed parameter (τ_n) space is hit. Although this feature in the analytic DTDs is purely numerical, we do expect an abrupt change in the distribution at a delay time equal to the MS lifetime of the least massive secondary in successful SN Ia progenitors.

Inspection of Fig. 2 shows that the various models provide similar curves: the DTD features an early maximum and most events occur within ~ 1 Gyr from formation. At later epochs the DTD exhibits a steady decline with a pronounced downturn for the SD Chandra model. All distributions accommodate *prompt* and *tardy* events, but with a substantial continuity over the whole range of delay times; this follows from the assumption of continuous distributions over the relevant parameter space of masses and separa-

rations of SN Ia progenitors. In the next section these curves are compared with theoretical results in the literature.

2.3 Analytic DTDs and BPS results

In deriving the analytic DTDs described above one potentially important variable is neglected, i.e. the separation of the primordial binary A_0 . In order to provide a successful event, A_0 ought to range between a minimum and a maximum value, respectively to avoid premature merging, and secure interaction at all. As long as these limits do not depend on the component's masses, the shape of the DTD is not affected, and the limitation just reflects into the overall likelihood of the SN Ia event from a stellar population. However, the minimum and maximum initial separations tend to increase with the mass of the primary, because more massive stars have larger radii at all key points along evolution. Figures 1 to 4 in Iben and Tutukov (1987) well illustrate this point, also showing that, in general, the range of separations for a successful interaction widens as the primary mass grows. If the distribution of A_0 were flat, the more massive binaries would have then greater chance to provide SN Ia's; on the other hand, closer systems should be more abundant (Abt 1983), so that the more massive binaries also have a higher likelihood of premature merging. Therefore, it is not clear how the efficiency of SN Ia production from a binary of given (m_1, m_2) varies with the system separation. The comparison of the analytic DTDs with results from BPS helps understanding whether or not the analytic functions capture the most important astrophysical parameters.

In Paper I the analytic DTDs are compared to the BPS results of Yungelson & Livio (2000): consistency is found for the Sub-Chandra and for the DD-Chandra cases, when accounting for the limits on m_1 and m_2 adopted by the authors. The comparison between the DTDs of the SD-Chandra channel is hampered by the narrowness of the range of secondary masses in systems which provide SN Ia through the H-rich SD path in the Yungelson & Livio (2000) simulations. Actually, the conditions for stable mass transfer and/or a successful growth to the Chandrasekhar limit of the H-accreting CO WD are often found to hold only within a very restricted range of m_2 . The analytic DTDs do not incorporate constraints on the mass transfer rate, but the mass range covered by the components of successful systems is to be considered as a parameter.

Hachisu, Kato & Nomoto (2008) present the DTD for the SD-Chandra scenario taking into account the effect of a radiative wind from the accreting WD which stabilises the mass transfer (Hachisu, Kato & Nomoto 1996), favouring the WD mass growth. Although their computation is not a BPS simulation, the DTD is obtained by integrating the distributions over the appropriate range in the parameter space (m_1, m_2, A_0) which leads to successful explosions, according to their modelling of the evolution of CO WDs accreting from a MS and from a RG companion. It is instructive to compare their derived DTD with the Paper I analytical distributions. Let's first consider the WD+RG channel: Hachisu et al. (2008) find it active for $m_2 \lesssim 3 M_\odot$, and indeed the corresponding DTD is populated at $\tau \gtrsim 0.4$ Gyr; its DTD is marked by two cusps, at 1.6 and 12.6 Gyr. Given the wide bins of delay time in the Hachisu et al. (2008) computation, the position of the cusps are consistent with those on the solid line in Fig. 1. For the same choice of IMF (Salpeter) and distribution of mass ratios (flat) as in Fig. 1, the slope of the DTD between the two cusps (in logarithmic units) is -1.4, perfectly consistent with the analytic DTD. The WD+MS channel is found active for $2 \lesssim m_2/M_\odot \lesssim 6$ and, in fact, the relative

DTD goes to zero in the vicinity of $\tau = 1$ Gyr; the slope is ~ -1.4 , much steeper than the slope of the WD formation rate (dashed line in Fig. 1) in the same range of delay times, which is ~ -0.5 . This may signal that the distribution of the separations is important in shaping the DTD of the WD+MS channel, favouring SN Ia events in the more massive binaries.

The DTD from the WD+MS channel has also been presented by Han & Podsiadlowski (2004), as derived with their BPS code. The resulting DTD is a rather narrow, almost flat distribution, within limits which depend on the parameter for CE efficiency. A similar shape is found for the WD+MS channel in Meng, Chen & Han (2009). The limits are consistent with the MS lifetime of the most and least massive secondary in SN Ia progenitors through this channel, which are found confined between ~ 3 and $\sim 2 M_\odot$. These DTDs are quite different from those in Hachisu et al. (2008), possibly because of the use of a different technique and of different details in the assumptions. Therefore, the shape of the DTD for the WD+MS channel seems rather sensitive to the adopted approach.

DTDs based on BPS calculations have been presented by Belczynski, Bulik & Ruiter (2005) and more recently by Ruiter et al. (2009). Since the former models include Sub-Chandra explosions, which actually provided the majority of events (Ruiter et al. 2009), their comparison with the analytic DTDs is not practical. More similar are the SN Ia production channels in the models presented in Ruiter et al. (2009), which include only Chandra exploders, from DD progenitors (DDS), H-rich SD Chandra progenitors (SDS), and CO WDs accreting Helium via stable RLOf, either from a non degenerate or from a degenerate companion (AM CVn). The DTD for the DDS channel is very similar to the analytic function, with a logarithmic slope of ≈ -1 . Notice that when the efficiency of the CE phase is reduced ($\alpha_{CE}=0.5$) the DTD of the DDS channel is found steeper, as a consequence of the smaller orbital separations of the DD systems when they emerge from the CE. The same effect can be obtained by varying the parameter β_g or β_a in the analytic DTDs. The comparison with the BPS results for the SD channel is more complicated, due to its splitting into the two classes SDS and AM CVn in Ruiter et al. (2009). However, the BPS DTD seems much flatter than the analytic DTD in the range of delay times between 3 and 6 Gyr, and lacks the dramatic drop at late epochs. Since the clock of the explosion is the evolutionary lifetime of the secondary (also in the BPS simulations), it seems that the envelope mass of the secondary has little influence on the efficiency of the production of Chandra explosions in the SDS channel, in the simulations by Ruiter et al. (2009).

To summarise, the comparison of the analytic curves with other results in the literature shows that the limits on the component's masses play a crucial role in shaping the DTD, while the effects of the limits on A_0 are much less evident, except perhaps for the WD+MS progenitors. While the analytic DTDs for the DD models match well the BPS results, the DTD of SD models turns out appreciably different. It seems however that diverse realisations are obtained by different authors, both for the range of m_2 of SN Ia progenitors, and for the DTD slope. These differences likely reflect the sensitivity of the results of the systems' evolution to details in the prescriptions adopted for the simulations.

3 EFFECT OF PARAMETERS

By construction, the analytic DTDs have a built in parametrisation of some astrophysical variables related to the binary population and

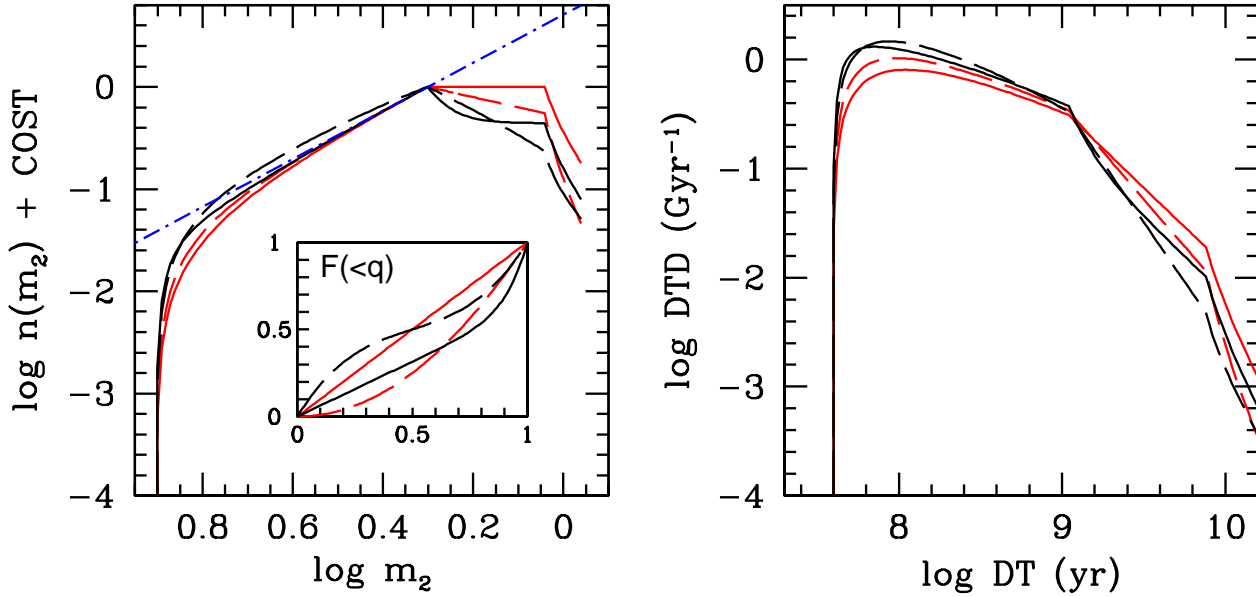


Figure 3. Effect of the distribution of the mass ratios on the mass distribution of the secondaries (left) and on the DTD (right) of SN Ia from the SD-Chandra channel. All curves assume $(m_1, m_2) \leq 8M_\odot$, and a Salpeter distribution for the primary masses. Red lines assume $f(q) \propto q^\gamma$ with $\gamma = 0$ (solid) and 1 (dashed). Black lines assume Eq.(2) (solid) and (3) (dashed). The cumulative distributions of q are shown in the inset (left panel). The dashed-dotted blue line in the left panel shows a Salpeter distribution: with respect to this line, $n(m_2)$ is underpopulated at both the high and the low mass end, because of the requirements on the binary system SNIa progenitor. The deficiency at the high mass end is due to the upper limit of $8M_\odot$ on the primary mass; at the low mass end, instead, it is due to the lower limit on the mass of the WD.

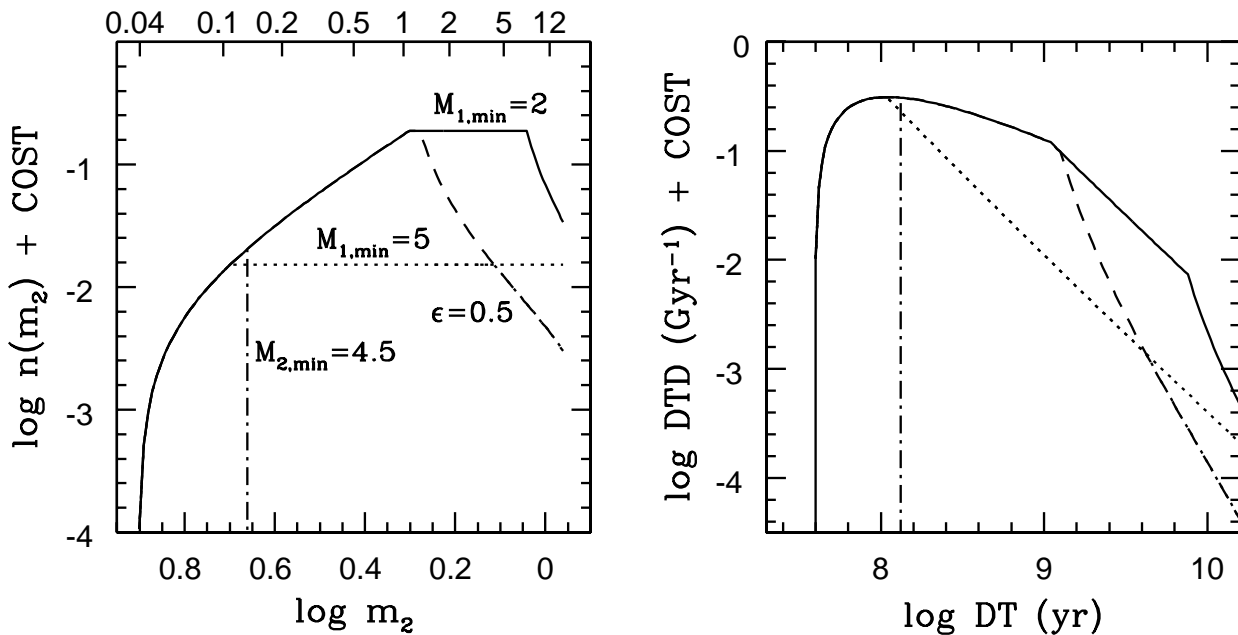


Figure 4. Distribution of the secondaries (left) and on the DTD (right) of SN Ia from the SD-Chandra channel for a flat $f(q)$. All curves assume $(m_1, m_2) \leq 8M_\odot$, but differ in the value of other parameters: the solid and dotted lines assume a minimum m_1 of 2 and $5M_\odot$ respectively, no lower limit on m_2 , and $\epsilon = 1$; the dashed line assumes the same limits as the solid line, but $\epsilon = 0.5$; the dot dashed lines assumes a minimum m_2 of $4.5M_\odot$. The line encoding is the same in the two panels. The top axis in the left panel is labelled with the MS lifetime of the evolving secondary, in Gyr.

to the progenitor’s model. In addition, they are constructed by relating the delay time to the exploding system, so that systematic variations of the properties of SN Ia progenitors with the delay time can be envisaged. In this section these issues are illustrated for the Single and the Double Degenerates.

3.1 Single Degenerates

The curves in Fig. 1 are constructed upon specification of: the slope of the mass distribution of the primaries (α), the distribution of the mass ratios ($f(q)$), the mass range of the primaries and of the secondaries in successful systems. An additional parameter is the accretion efficiency ϵ , namely the fraction of the envelope mass of the secondary which is actually accreted by the primary. The solid curve in Fig. 1 assumes $\alpha = 2.35$ (as all other DTDs in this paper), a flat distribution of the mass ratios, the maximum possible range for m_1 and m_2 , and that the whole envelope of the secondary is available for the WD to grow up to the Chandrasekhar limit ($\epsilon = 1$). The same curve is reproduced as a solid line in Fig. 4. The dependence on α and $f(q)$ have been illustrated in Paper I: basically, any combination which favours low mass secondaries leads to a larger fraction of late epoch events. In Paper I it is also shown that when using the alternative algorithm adopted in Greggio & Renzini (1983) to derive $n(m_2)$, the fraction of low mass secondaries is enhanced, for a given IMF and distribution of the mass ratios².

Empirical determinations of the distribution of the mass ratios in binaries are subject to considerable observational biases (see e.g. Kouwenhoven et al. 2007). Most binary population synthesis computations assume a flat distribution; on the other hand, there is growing evidence for a prominent population of twins among close binaries, which could enhance the fraction of systems with short delay times (Pinsonneault & Stanek (2006) and references therein). Fig. 3 shows the distribution of the secondary masses and the ensuing DTDs under various assumptions for $f(q)$. In particular, the two black lines assume a distribution of the mass ratios made of two components: the solid line adopts

$$f(q) = 0.63 + 2.42 \times (q/0.95)^{10} \quad (2)$$

which is a flat distribution up to $q \simeq 0.8$, plus a prominent population of twins. This function roughly fits the distribution in Pinsonneault & Stanek (2006) for $q \gtrsim 0.5$. The dashed black line adopts

$$f(q) = 6.9q^2 - 6.9q + 2.15 \quad (3)$$

which roughly reproduces Trimble (2008)’s results, with a strong component at the lowest and highest values of the mass ratio, and a minimum at $q = 0.5$. Clearly, the distributions with a high proportion of twins (the two dashed lines and the solid black line) provide DTDs which are relatively more populated at the short delay times. The effect however does not appear dramatic, nor does a two components $f(q)$, as in Eqs. (2) and (3), reflect into a two components DTD. All following computations adopt a flat distribution of the mass ratios, an option which maximises the fraction of late epoch explosions. This will be taken into account when discussing the results.

Similar to Fig. 3, Fig. 4 illustrates the effect of varying the

other parameters. The dashed curves assume the same limits for the masses of the components as the solid curve, but $\epsilon = 0.5$ for all systems. The possibility of accreting only half of the envelope of the secondary has a dramatic impact on the number of systems with a low mass secondary which manage a Chandra explosion; correspondingly, the DTD drops rapidly off at delay times slightly over a Gyr. This makes it difficult for the SD channel to account for a sustained SN Ia rate at long delay times: for example, at an age of 13 Gyr, the stars evolving off the MS for a single burst stellar population have a mass of $\sim 0.9M_\odot$. With a core mass of $0.3M_\odot$, only $0.6M_\odot$ are available for accretion onto the companion WD, and, if $\epsilon = 0.5$, the Chandrasekhar limit can be met only starting with a CO WD heavier than $1.1M_\odot$. Therefore, the range of suitable primary masses is exceedingly small ($7 \lesssim m_1 \lesssim 8$). The dotted curves in Fig. 4 show the effect of implementing a more severe lower limit to m_1 : $5M_\odot$ instead of $2M_\odot$, corresponding to SN Ia’s arising only from CO WDs more massive than $\sim 0.9M_\odot$. In this case, $n(m_2)$ gets substantially deprived of systems as soon as m_2 drops below $5M_\odot$, and the DTD gets depressed at the corresponding MS lifetime ($\simeq 0.1$ Gyr); however the distribution remains wide, without strong discontinuities. A strong discontinuity may instead be obtained by implementing a dramatic change in SN Ia production at some value of m_2 , due to the one to one correspondence between delay time and mass of the secondary in the SD model. In particular, a lower limit on m_2 has the effect of vanishing the DTD at delays longer than the MS lifetime of such stellar mass. The dashed-dotted lines in Fig. 4 show the effect of adopting a lower limit of $4.5M_\odot$ to the secondaries in SN Ia progenitors, mimicking what happens for the SD Helium star channel which requires massive secondaries. Notice that, according to Wang et al. (2009), the secondary mass in such SN Ia progenitors ought to be larger than $5.6M_\odot$, implying a drop off in the DTD at ~ 80 Myr.

I turn now to consider some properties of the exploding WD which are predicted to vary systematically with the delay time in the context of the SD model. Lesaffre et al. (2006) presents a systematic study of the sensitivity of ignition conditions for H-rich Chandra SD exploders on various properties of the progenitor. These authors find that the more massive and/or the cooler the CO WD when accretion starts, the higher the central density at ignition. While it is not clear whether this leads to a larger or lower mass of synthesised ^{56}Ni , a systematic variation of ignition density could translate into a systematic variation of the properties of the SN Ia explosions. It is thus interesting to analyse how the initial mass of the CO WD and its cooling time vary with the delay time.

The top panel in Fig. 5 shows the range for the initial WD mass of SN Ia progenitors as function of the delay time, for a few choices of the relevant parameters. The limits on the WD mass follow from the limits on m_1 through the adopted initial-final mass relation ($M_{\text{wd}} = 0.6 + 0.1 \times (M - 2)$) as in Paper I). The maximum value of the primary mass is $8M_\odot$ irrespective of the delay time; the lower limit is given by m_2 (function of τ), or higher, either because a fixed limit on m_1 sets in ($2M_\odot$ for the solid line, $5M_\odot$ for the dotted line), or, at late delay times, because of the need of securing a Chandrasekhar mass at explosion. Correspondingly, the range of initial mass for the CO WD is small at short delays (only massive binaries have had time to evolve), but it rapidly increases with τ ; at intermediate delay times the range of initial WD mass is maximum, but at late delays it shrinks, because a massive primary is required to accomplish a Chandra explosion. The latter regime sets in earlier for a less efficient accretion (e.g. the dashed curve).

The bottom panel of Fig. 5 shows the range of cooling times of the CO WD, i.e. the time elapsed between its the formation and

² Notice that the Greggio & Renzini (1983) formalism assumes power law distributions for the total binary mass M_B and for the ratio of m_2 to M_B , so that the same IMF slope and distribution of the mass ratios have different meanings in the two approaches.

the start of the accretion phase. In this time interval the WD cools, becomes progressively more degenerate, and other processes like C and O separation and crystallisation (e.g. Salaris et al. 2000) set in. The path towards explosion, and the explosion outcome critically depend on the initial structure of the CO WD, or, in turn, on the cooling time. For example, the C and O relative diffusion may affect the amount of synthesised ^{56}Ni , hence the light curve. On average, the cooling time increases with the delay time, and its range reaches a maximum at $\tau \approx 1$ Gyr, to become smaller at longer τ . Most noticeably, the cooling time is very long, up to several Gyr, for most values of delay time.

To summarise, some dispersion in both parameters is present at all delay times, but for early events this dispersion is more pronounced. Qualitatively, then, we may expect more diversity in SN Ia events from younger stellar populations. On the other hand, at short delays the CO WD at the beginning of the accretion phase is (on average) more massive and younger; thus, due to compensating effects, the trend of ignition density with delay time could be relatively weak. Conversely, at long delay times the mass and cooling age of the CO WD both increase with τ , so that the ignition density should increase systematically. It is important to notice that very long cooling times, of few to several Gyrs, characterise most of the events, whereas Lesaffre et al. (2006) models include cooling ages of ≈ 1 Gyr at most. As the delay time increases, the CO WD has time to become more and more degenerate before the start of the accretion phase. The evolution of the WD structure during the accretion phase, as well as the outcome of C ignition under extremely degenerate conditions are important questions which need more attention than currently present in the literature.

3.2 Double Degenerates

Due to the relatively restricted mass range of the binary components (i.e. from 2 to $8 M_{\odot}$) in the DD model, the DTD is not very sensitive to the IMF slope and to the distribution of the mass ratios, whereas the main parameters controlling its shape are the maximum delay due to the MS evolution of the secondary ($\tau_{n,x}$), and the shape of the distribution of the separations. The parameter $\tau_{n,x}$ is the evolutionary lifetime of the least massive secondary in successful SN Ia progenitors: the heavier this limit is, the earlier the position of the cusp in the DTD for both CLOSE and WIDE DDs. The shape of the distribution of the separations of the DD systems controls instead the overall slope of the decline as the delay time grows: if most systems are born close, most events have a short τ_{GW} and the DTD declines faster. Fig. 6 shows these dependences; notice that the DTDs are not normalised to 1 for illustrative purposes. The three values of $\tau_{n,x}$ which characterise the curves in the left panels correspond to a minimum mass of the secondary in successful systems of 2 (solid), 2.5 (dashed) and $3 M_{\odot}$ (dot-dashed): for normalised DTDs, the fraction of early events is higher when this minimum mass is larger. The curves in the right panels all adopt a minimum m_2 of $3 M_{\odot}$, but different distributions of the separations, as described by the parameters β_a and β_g for the WIDE and CLOSE cases respectively. Although the two parameters are defined in a different way (see Sect. 2.2), the smaller their values the larger the fraction of systems with small separation A , and the three curves correspond to a flat distribution (solid), a distribution more populated at small (dot-dashed) and at large (dashed) separations. For all the values of the β parameters considered here, the DTD declines towards long delay times, but the slope is milder when β_a or β_g are larger, since in this case more systems have a long gravita-

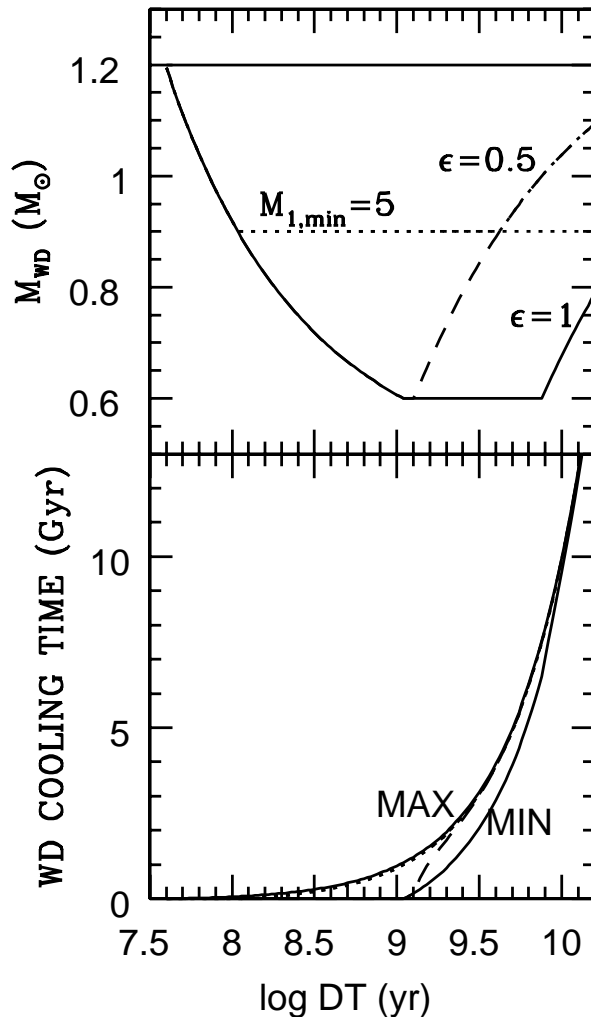


Figure 5. SD model: systematic variation with the delay time of the mass range (top) and of the cooling time range (bottom) of the CO WD when accretion starts. The different curves refer to different choices of the minimum m_1 and of the parameter ϵ with the same line encoding as in Fig. 4.

tional wave radiation delay. Consequently, the higher β_a or β_g , the larger the fraction of events at late epochs.

Some other parameters have been fixed to derive the DTDs shown in Fig. 6: the minimum evolutionary lifetime of the secondary ($\tau_{n,0}$) and the minimum τ_{GW} ($\tau_{\text{GW},0}$) in successful systems. The adopted values are $(\tau_{n,0}, \tau_{\text{GW},0}) = (0.04, 0.001)$ Gyr, and correspond, respectively, to assuming that (i) the most massive secondary in SN Ia progenitors is an $8 M_{\odot}$ star, and (ii) that the minimum delay due to gravitational wave radiation is negligibly small³. On the other hand, the upper limit to m_2 could be lower than $8 M_{\odot}$, if, e.g., systems with massive secondaries feed the SD, rather than the DD channel. Likewise, a significant lower limit to τ_{GW} could be realised in nature, if, e.g., DD systems which are born too close, or are too massive, undergo an accretion induced collapse rather than a SN Ia explosion. Both alternatives deprive the DTD of early events, while maintaining the population at long delay times. Fig. 7 shows the effect of varying separately $\tau_{n,0}$ and $\tau_{\text{GW},0}$ for the CLOSE

³ The value of 1 Myr is imposed for numerical reasons.

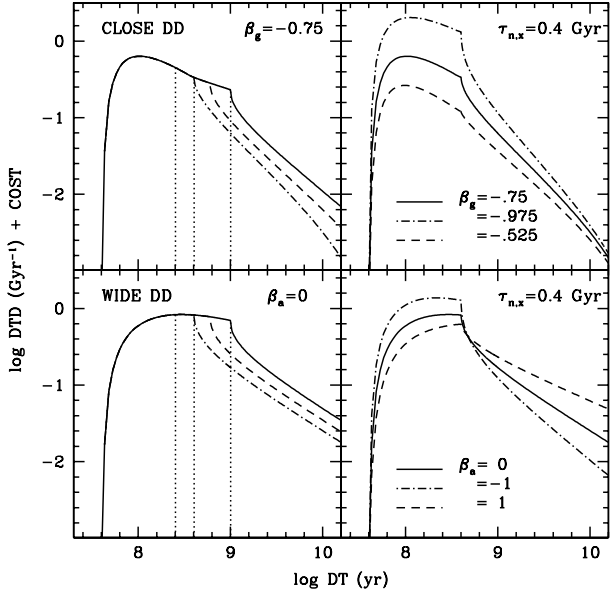


Figure 6. Effect of the main parameters on the DTD of DD CLOSE (upper panels) and DD WIDE (lower panels) models. The left panels show the dependence on the maximum evolutionary lifetime of the secondary: $\tau_{n,x}=1$ (solid), 0.6 (dashed) and 0.4 (dash-dotted) Gyr, for the labelled values of β_a and β_g . The right panels show the dependence on the distribution of the separations as labelled. Notice that the DTDs are not normalised to unity for better illustration.

and the WIDE DD models: some DTDs assume a nominal $\tau_{GW,0}$ coupled to $\tau_{n,0}=0.1$ and 0.15 Gyr (corresponding to a minimum m_2 of 5.2 and 4.3 M_\odot respectively); some DTDs assume the default $\tau_{n,0}=0.04$ Gyr coupled to $\tau_{GW,0}=0.1$ and 0.2 Gyr. The latter limits correspond to systems with a separation of 1 R_\odot and masses $M_{DD}=2$ and 1.4 M_\odot respectively. In all cases the DTD is deprived of events with delay times shorter than $(\tau_{n,0} + \tau_{GW,0})$, but the overall shape is not much affected, though for the WIDE DD case a higher $\tau_{GW,0}$ spreads the DTD toward longer delay times. It is also worth noting that the cusp in all DTDs is actually located at $\tau = \tau_{n,x} + \tau_{GW,0}$: indeed, when the minimum gravitational wave radiation delay is non negligible, the limit $\tau_n \leq \tau_{n,x}$ corresponds to a discontinuity in the parameter space for τ located at $\tau_{n,x} + \tau_{GW,0}$.

For the DD channel, at each delay time the events come from systems with a range of τ_n (e.g. $\tau_{n,0} \leq \tau_n \leq \tau - \tau_{GW,0}$) and a corresponding range of τ_{GW} . Therefore, systems with different masses of the components and different separations end up exploding at the same delay time, so that the occurrence of a significant discontinuity in the DTD at a particular delay time is unlikely. Similarly, there is no one to one correspondence between the delay time and the mass of any of the WD components; however there is a trend of high mass binaries providing preferentially explosions at early delays.

The diversity of the SN Ia light curves could be due to the range of total mass M_{DD} if, e.g., the amount of ^{56}Ni produced in the event was correlated to the total mass of the exploding system. For example, the extra mass ($M_{DD} - 1.4$) could act as a *tamper* in the explosion, i.e. inertially containing it a little longer, and lead to a higher production of ^{56}Ni . Although this possibility has not been explored with theoretical models, it is worth noting that the remarkable event SNLS-03D3bb was both over-luminous and Super-

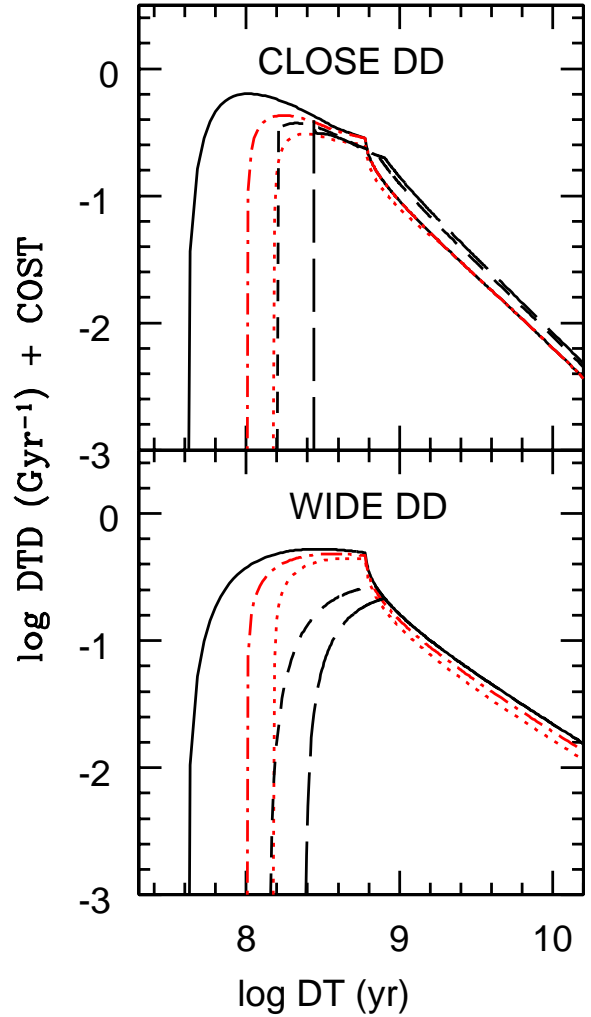


Figure 7. Effect of varying the minimum evolutionary lifetime ($\tau_{n,0}$) and gravitational wave radiation delay ($\tau_{GW,0}$) in SN Ia progenitor systems for DD CLOSE (top) and WIDE (bottom) models. The line-types encodes the values of $(\tau_{n,0}, \tau_{GW,0}) = (0.04, 0.001)$ (solid), $(0.1, 0.001)$ (dot-dashed, red), $(0.15, 0.001)$ (dotted, red), $(0.04, 0.1)$ (short dashed), $(0.04, 0.2)$ (long dashed). All curves assume a minimum m_2 of 2.5 M_\odot , and a flat distribution of A .

Chandrasekhar (Howell et al. 2006). Fig. 8 illustrates the expected trend of the range of M_{DD} with the delay time. The lower limit represents the less massive systems which have had time to evolve at a given τ , i.e. binaries in which m_2 is the evolutionary mass with lifetime equal to τ , and $m_1 = m_2$. For a negligible value of $\tau_{GW,0}$, some of these systems merge at a delay time τ . If the close binary evolution ends up with a wide range of separations of the DD systems irrespective of the components' masses, the maximum M_{DD} is the remnant of the $(8+8) M_\odot$ systems, i.e. $M_{DD} = (1.2+1.2) M_\odot$, independent of τ . It will be in fact always possible to find a massive system wide enough, so that the gravitational wave radiation delay equals $\tau - \tau_n$. This upper limit could be appropriate for the WIDE DD case (dashed line). However, massive binaries, which end up with massive remnants, also undergo a severe shrinkage, especially in the CLOSE DD case. Therefore, high M_{DD} will be associated to short τ_{GW} , and short total delays in general; this introduces a trend for the upper limit to M_{DD} with τ . The solid line in Fig. 8 illustrates

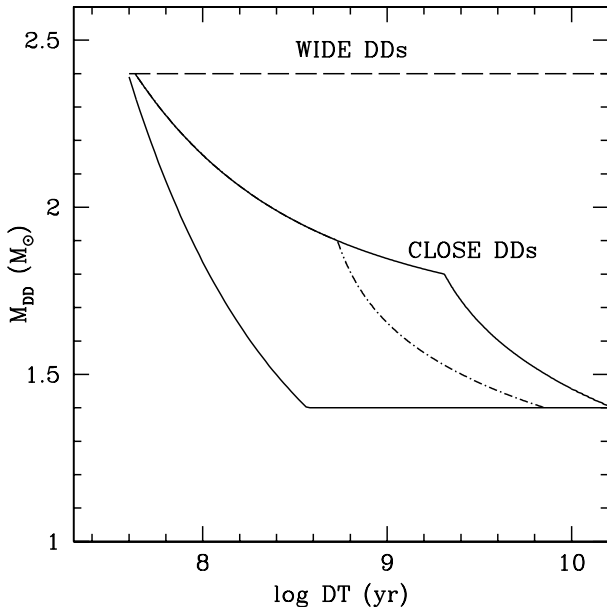


Figure 8. Illustration of the dependence on delay time of the range of DD systems total masses for the WIDE (dashed) and the CLOSE channels. For the latter, the upper limit shown as a solid (dash-dotted) line refers to a minimum secondary mass of 2 (3) M_{\odot} in SN Ia progenitors. A maximum m_2 of $8 M_{\odot}$ and a negligible lower limit for τ_{GW} have been adopted. For delay times longer than ~ 0.35 Gyr the lower limit is given by the Chandrasekhar mass.

this effect, and has been computed by applying the α_{CE} recipe to two consecutive RLOf episodes. The exact location of this upper limit depends on various parameters (e.g. α_{CE} , maximum separation of the interacting systems, initial-final mass relation), but the general trend is realistic. In fact, at each delay time, the maximum M_{DD} is realised in systems with maximum remnants from m_1 and m_2 which merge within $\tau_{\text{GW}} = \tau - \tau_{\text{n}}(m_2)$. Since τ_{GW} is shorter in more massive systems, due to its explicit dependence on M_{DD} , as well as to the higher shrinkage, the above condition is met for certain values of m_1 and m_2 below their maximum values of $8 M_{\odot}$. The calculation shows that, as the total delay time grows, the condition above is first met with the maximum m_1 ($8 M_{\odot}$) in combination with a progressively less massive secondary, until the latter reaches the lower limit on m_2 (e.g. $2 M_{\odot}$) adopted for the DD progenitors. At delay times longer than this the maximum M_{DD} is realised in systems with $m_2 = 2 M_{\odot}$ and a progressively lighter maximum primary. The transition between the two regimes is marked by the cusp in Fig. 8.

To summarise, for the WIDE DD case we expect a wide range of M_{DD} at any delay time, and virtually no trend for the average mass of the exploding WD with the age of the parent galaxy. Instead in the CLOSE DD case we expect a definite trend of decreasing average M_{DD} with increasing delay time, i.e. with increasing average age of the parent population. In addition, the range of M_{DD} in SN Ia progenitors should become narrower in old systems, where the events should basically come from M_{DD} close to the Chandrasekhar mass.

4 MIXED MODELS

As shown in the previous sections, the different channels for SN Ia production are in principle capable to provide both *prompt* and *tardy* events, as required by the data. Moreover, for all channels the DTD favours early events, so that the SN Ia rate per unit mass in young stellar systems is expected higher than in old ones, again as required by the observations. Although the fraction of early explosions is different for the different channels, and within the same channel it depends on the astrophysical parameters which characterise the progenitor systems, each model is compatible with the decreasing rate per unit mass going from late to early type galaxies. On the other hand, there's no real need to view the various models as mutually exclusive, and both SD and DD paths could well be realised in nature. From the stellar evolution point of view, the SD channel has more difficulty to produce Chandrasekhar explosions at very late epochs past star formation, because of the small mass reservoir from the donor; the DD channel instead, can provide events at delay times exceeding the Hubble time due to the possibility of realising very long τ_{GW} . Therefore, rather than considering the two channels as mutually exclusive, it seems wiser to construct a mixed model, in which both SD and DD events concur to the SN Ia explosion. Among the many possible combinations, I consider two extreme hypothesis: the *Solomonic* mix, in which both SD and DD channels contribute half of the total events within 13 Gyr; the *Segregated* mix, in which the SD explosions provide the early events, while the DD channel feeds all the remaining delay times. Although many other combinations are possible, it is instructive to see how these choices, which maximise the contribution of the two channels, impact on the DTD, and explore how the mix may be constrained by the observations.

Fig. 9 shows the Solomonic (left) and the Segregated (right) mixtures obtained with the particular choice of parameters for the individual channels as described in the caption. The Solomonic mix is characterised by a DTD which is very similar to each of the SD and DD models used to construct it; the only significant feature is the intermediate slope of the decline at very late delays, where the number of events is kept relatively high due to the contribution from the DD channel. This characteristic is relevant for the SN Ia rate in the oldest galaxies, as will be illustrated later on. At each delay time, the ratio between DD and SD explosions varies, but it keeps within a factor of 2 over almost the whole range of τ : only for $\tau \geq 9$ Gyr does the DD channel definitely prevail. This kind of mixture and its evolution over cosmic time has been studied in Greggio et al. (2008). In general, for the Solomonic mixture, the majority of SN Ia events in early type galaxies should come from DD systems with M_{DD} close to the Chandrasekhar mass. The events in late type galaxies, instead, should come from both channels and may include super-Chandra explosions from DD progenitors.

The Segregated mix assumes that systems with $m_2 \geq 5 M_{\odot}$ feed the SD channel, while systems hosting less massive secondaries undergo CE evolution at the second RLOf, to become DDs, hence the discontinuity at 0.1 Gyr. This combination mimics the DTD proposed by Mannucci et al. (2006) to explain the high SN Ia rate in radio loud Ellipticals as due to a recent SF episode in combination with a high fraction of *prompt* explosions. Actually, if this were the case, the excess of 7 Ia events in the radio loud Ellipticals would imply that ~ 14 CC SNe should have been detected in the same sample, while none was observed (Greggio et al. 2008). It is anyway instructive to consider this DTD as an example of a distribution with a high fraction of events at very short delay times; here

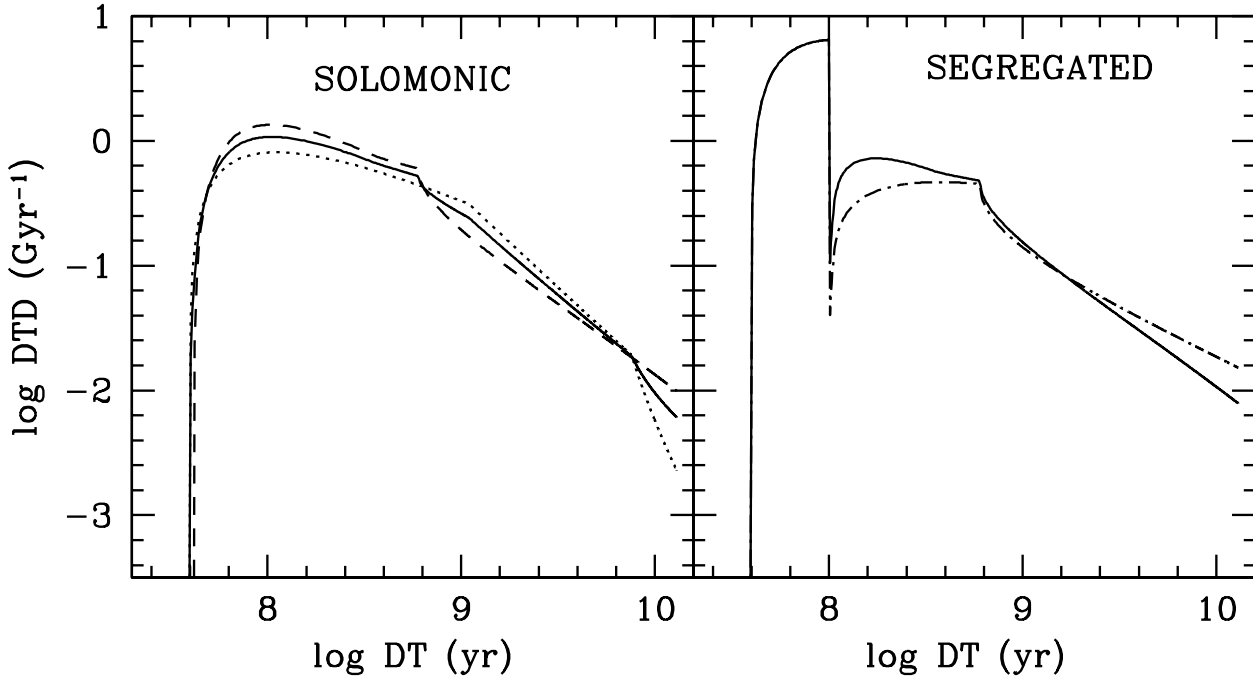


Figure 9. DTDs for mixed models. Left: the DTD of SD Chandra explosions in Fig. 1 (dotted line) is combined with the DTD of a DD-CLOSE model with minimum secondary mass of $2.5 M_{\odot}$ and a flat distribution of A (dashed) to construct the Solomonomic mixture, in which 50 % of the total events within 13 Gyr come from either channel. Right: the events at delay times shorter than 0.1 Gyr come from SD explosions, while those at longer delay times come from the DD-CLOSE (solid) or DD-WIDE (dot-dashed) evolutionary channels, both with minimum m_2 of $2.5 M_{\odot}$ and a flat distribution of A . The events from the SD channel amount to 30 % of the total within 13 Gyr.

a fraction of 30 % *prompt* events was chosen following the indications from chemical evolution models by Matteucci et al. (2006). In this option, all events in early type galaxies come from the DD channel, while in galaxies with ongoing star formation we get a mixture of SD and DD explosions. In most cases, the two channels will be providing events with similar probability: in fact the SN Ia rate in a galaxy ~ 13 Gyr after the beginning of star formation is given by:

$$\dot{n}_{Ia}(13) = k_{Ia} \times \left(\psi_c \int_0^{0.1} f_{Ia}(\tau) d\tau + \psi_p \int_{0.1}^{13} f_{Ia}(\tau) d\tau \right) \quad (4)$$

where k_{Ia} is the number of SN Ia from a stellar population of unitary mass (or SN Ia productivity), and ψ_c and ψ_p are the (f_{Ia} weighted) average SF rates over, respectively, the last 0.1 Gyr and from 0.1 up to 13 Gyr ago. Equation (4) explicitly shows the two contributions of *prompt* and *tardy* components of the DTD: if their ratio is of 0.3 to 0.7, in order to have an equal probability to realise SD or DD explosions it suffice that the current SF rate exceeds the average SF rate in the past by a factor of ~ 2 .

To summarise, both the Solomonomic and the Segregated mixtures provide SD and DD explosions in virtually all galaxy types, but in the very old galaxies, where (almost) all events should come from the DD channel. It is worth noting that this conclusion only applies to Chandra explosions, since Sub-Chandra events could be common at very late delay times both in the Single and Double Degenerate scenarios.

The scaling of the SN Ia rate in different stellar systems offers the opportunity of constraining the DTD, hence the SN Ia pro-

genitor model (e.g. Paper I, Mannucci et al. 2006; Blanc & Greggio 2008). To this end I consider two sets of data: (i) the relation between the SN Ia rate per unit luminosity and the morphological type of the parent galaxy (Greggio & Cappellaro 2009, hereinafter GC09) and (ii) the relation between the SN Ia rate per unit mass and the specific SF rate (SSFR) of the parent galaxy (Sullivan et al. 2006). Both relations (i) and (ii) basically stem from DTD being more populated at early delay times: as a consequence, the rate per unit mass is higher the younger the stellar system. A later galaxy type and/or a higher specific SF rate correspond to a larger fraction of young stars, hence a higher SN Ia rate per unit mass, or per unit luminosity, as far as luminosity traces the stellar mass. Nonetheless the two observational relations are largely independent (i) because of the different galaxy sample, and (ii) because of the different normalisation of the SN Ia rate, and different galaxy age tracer. Therefore, they yield complementary information on the DTD. In the next sections, the quantitative fit of the two relations is attempted separately.

4.1 Rates as function of galaxy type

The indication that late type galaxies are more efficient in producing SN Ia events goes back to Tammann (1978), and was interpreted as due to a DTD more populated at short delay times already by Oemler & Tinsley (1979) and Greggio & Renzini (1983). Since then, this observational feature has been put on firm grounds as a correlation between the SN Ia rate per unit B-band luminos-

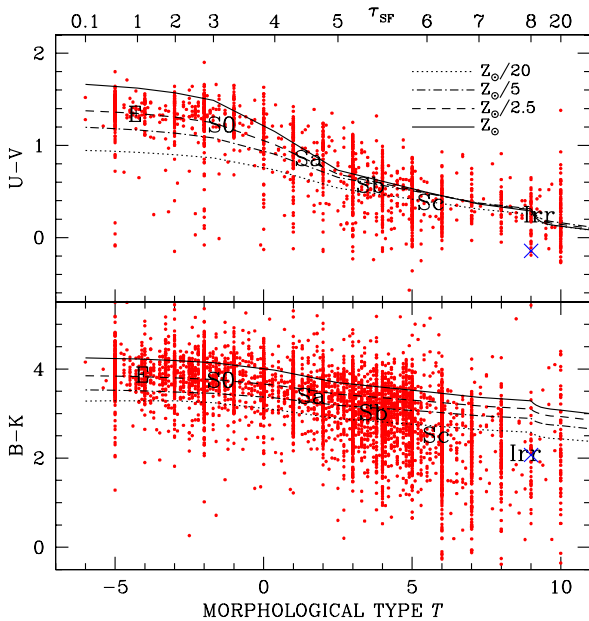


Figure 10. Calibration of the parameter τ_{SF} of the SF rate versus morphological galaxy type. The red dots show the galaxies of the Cappellaro et al. (1999) sample; the letters show the average location in color and type of the labelled galaxy class. The lines connect galaxy models obtained convolving the SF rate given by Eq. (5) with the τ_{SF} value labelled on the top axis (in Gyr) with simple stellar population (SSP) models. The latter were derived using the CMD tool (version 2.2) posted on the web (<http://stev.oapd.inaf.it/cgi-bin/cmd>), with the following input: Marigo et al. (2008) set of tracks; Maíz Appellániz (2006) and Bessell (1990) photometric system; no circumstellar dust and no extinction; Salpeter IMF. The line type encodes the metallicity of the SSP models, as labelled. The blue crosses shows the colors of a model with an exponentially increasing SF rate in the last 13 Gyr, and an e-folding time of 1 Gyr, assumed to represent a bursting galaxy.

ity (rate in SNU's⁴) with the $U - V$ colour of the parent galaxy (Cappellaro, Evans & Turatto 1999), and a correlation between the rate per unit K band luminosity (rate in SNUK's) and the $B - K$ colour of the parent galaxy (Mannucci et al. 2005). Both correlations are based on the (Cappellaro et al. 1999) sample of (nearby) galaxies. Mannucci et al. (2005) also derived the rate per unit mass (rate in SNUM's) as a function of the parent galaxy $B - K$ colour, later used in Paper I and in Mannucci et al. (2006) to derive clues on the characteristics of the DTD. In particular, Paper I found that both CLOSE and WIDE DD models could explain the data, provided that the DTD slope was neither very flat nor very steep. However, the rate in SNUM's relies on theoretical models which are needed to convert the galaxies K-band luminosities into their mass; therefore the purely *observed* relations involve the rates per unit luminosities. The attempt to account for both Cappellaro et al. (1999) and Mannucci et al. (2005) trends of the rates in SNU's and SNUK's with the parent galaxy $U - V$ and $B - K$ colors fails (GC09), with the rate per unit L_B requiring a flatter DTD than the rate per unit L_K . This is because the slope of the observed correlations depend on both the DTD and on the SF history assumed to model the galaxies. To improve on the description of the latter, GC09 constrained

the sample galaxies to be represented by the family of SF history laws adopted by Gavazzi et al. (2002):

$$\psi(t) = \frac{t}{\tau_{\text{SF}}} \exp\left(\frac{-t^2}{2\tau_{\text{SF}}^2}\right) \quad (5)$$

which peaks at progressively older ages as the parameter τ_{SF} decreases. A short τ_{SF} also implies a narrow age distribution, akin to early type galaxies, while for $\tau_{\text{SF}} \geq 13$ Gyr the SF rate monotonically increases up to the present, having adopted an age of 13 Gyr for all galaxies. A calibration of τ_{SF} versus the morphological galaxy type T (as given in the RC3 catalogue, de Vaucouleurs et al.

1991) was obtained by fitting the $U - V$ and $B - K$ colours of the sample galaxies. In this way theoretical SN Ia rates (in SNU's and in SNUK's) as a function of T could be computed and compared to the measured correlations. Such procedure has two advantages: the galaxies' SF history is constrained from their luminosity in four photometric bands, and the full sample of SN Ia events in Cappellaro et al. (1999) can be used to derive the rates in SNU's because all galaxies have a determined L_B and type T , while L_K is available for only a fraction of them.

Fig. 10 shows the calibration of the τ_{SF} parameter versus T : the average colors of E, S0, Sa, Sb and Sc galaxies are reproduced with respectively $\tau_{\text{SF}} \approx 1, 3, 4.5, 5.5$ and 6 Gyr. It also appears that late type galaxies are better reproduced with a lower metallicity than early types. Concerning Irregular galaxies, the models account well for their average $U - V$ color, but appear too red in $B - K$ compared to the data. This may result from an inadequate description of their SF history, which could be dominated by a current burst. The cross in Fig. 10 shows the location of a bursting model, which well reproduces the $B - K$ color of this galaxy type, but turns out too blue in $U - V$, hence not providing a satisfactory fit either. For all other galaxy types, however, the average colors are well reproduced by the adopted SF history law, which is used in the following to fit the correlation of the SNIa rate with T .

The black dots in Fig. 11 shows the SNIa rates as function of morphological type determined in GC09, while the star shows the rate determined for the merged class of early type galaxies (E and S0) in Cappellaro et al. (1999) (upper panel) and Mannucci et al. (2005) (lower panel). The latter value turns out higher than the rates determined by GC09 in the individual classes; this is mostly due to a (slightly) different binning of the parameter T which identifies the morphological types. Coloured lines in Fig. 11 show theoretical relations obtained with selected DTD models (see caption), meant to show the dependence on the main parameters. The models are computed adopting the correspondence between τ_{SF} and T just discussed, plus a relation between τ_{SF} and metallicity Z , with Z decreasing from 0.008 to 0.001 as τ_{SF} goes from 1 to 20. The crosses in Fig. 11 show the location of the bursting model (cross in Fig. 10).

It is worth emphasising that, rather than simulating a large population of individual objects, the approach here aims at describing the photometric properties and the SNIa rate of the *average* galaxy within each bin of T ; the morphological type is assumed to trace the age mixture in the galaxies, and describe its changes across the Hubble sequence.

The theoretical rates in Fig. 11 are computed as the product of the rate per unit mass and the mass-to-light ratio of the galaxy models:

$$\frac{\dot{n}_{\text{Ia}}(t)}{L_{B(K)}} = k_{\text{Ia}} \frac{\int_0^{13} \psi(13 - \tau) f_{\text{Ia}}(\tau) d\tau}{M_{\text{SF}}} \times \frac{M_{\text{SF}}}{\int_0^{13} \psi(13 - \tau) \mathcal{L}_{B(K)}(\tau) d\tau} \quad (6)$$

⁴ Supernovae rate units are SNU's, SNUK's and SNUM's, corresponding to events per century per $10^{10} L_{B,\odot}$, $L_{K,\odot}$ and M_\odot respectively.

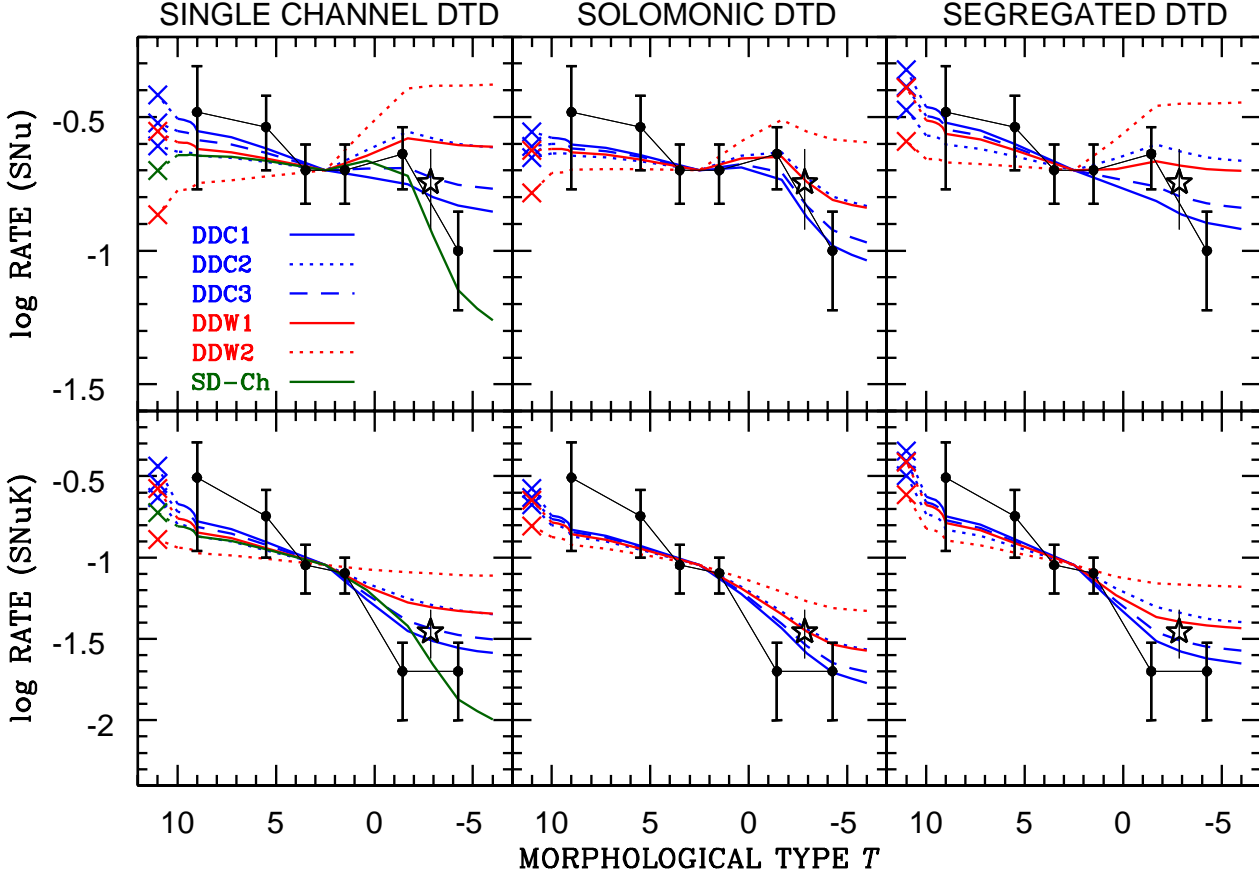


Figure 11. SN Ia rate per unit B (upper panels) and per unit K (lower panels) luminosity, as function of the morphological type of the parent galaxy. Black dots show the observed rates from Greggio & Cappellaro (2009); the stars shows the published rates for the E+S0 class; coloured lines show models calculated with different DTDs and the SF rate given by Eq.(5). Left panels: theoretical relations obtained with single channel DTDs. The SD Chandra (SD-Ch,m green line) model assumes a Salpeter distribution for m_1 , a flat distribution of the mass ratios, and an efficiency $\epsilon = 1$. Blue lines are obtained with DD-CLOSE models; DDC1 and DDC3 assume a distribution of separations skewed at small values, and differ for the minimum m_2 , respectively of 2.5 and 2 M_{\odot} ; DDC2 assumes a flat distribution of the separations and a minimum m_2 of 2.5 M_{\odot} . Red lines are obtained with DD-WIDE models, DDW1 and DDW2 being computed with the same choice of parameters as DDC1 and DDC2. Central and right panels: correlations obtained with mixed DTDs in the Solomonomic and Segregated flavours; colours and line types reflect the specific DD model used to construct the mixture with the encoding labelled in the top left panel. The coloured crosses show the rates for the bursting model in Fig. 10 put at an arbitrary value of T .

where $\mathcal{L}_{B(K)}$ are the light-to-mass ratios of simple stellar populations, either in the B or in the K band, as functions of age, and M_{SF} is the total mass transformed into stars (i.e. integral of $\psi(t)$) up to the current galaxy age, here assumed of 13 Gyr. When going from early to late type galaxies, the increase of the first factor (rate per unit mass) competes with the decrease of the second factor (mass to light ratio), which is more pronounced in the B, rather than K, band. This explains the large variation of the model rate in SNUK's compared to that in SNU's; it also explains why the rate in SNU's can even be predicted higher in early than in late type galaxies (see e.g. model DDW2).

The models are normalised to the observed value at $T = 3$, intermediate between Sa and Sb galaxies; the normalisation yields a value for k_{Ia} , i.e. the productivity of SN Ia from one unit mass stellar population, which depends on the assumed IMF. The observed rates imply $k_{Ia} \simeq 10^{-3} M_{\odot}^{-1}$ with relatively little dependence on the DTD or the photometric band, for the Salpeter IMF adopted in the CMD tool (i.e. $\phi(m) \propto m^{-2.35}$ down to 0.01 M_{\odot}). A bottom light

IMF, with $\phi(m) \propto m^{-1.3}$ between 0.1 and 0.5 M_{\odot} and a Salpeter slope above 0.5 M_{\odot} , would yield k_{Ia} values larger by a factor of ~ 3 . A detailed discussion of the uncertainty on k_{Ia} requires a thorough evaluation of the quality of the fits, which goes beyond the scope of this paper. It is however interesting to notice that this value of the SNIa productivity, compares well with the total Fe content of galaxy clusters. According to Renzini (2004) the Fe Mass-to-Light ratio of clusters is $M_{Fe}/L_B \sim 0.015$ in solar units, assuming a stellar mass-to-light ratio of $M_*/L_B \sim 3.5$. This value is appropriate for a bottom light IMF, for which the current mass in stars (at old ages) is ~ 0.6 of the total mass transformed into stars. Therefore, the Fe content in galaxy clusters requires an Fe productivity of $M_{Fe}/M_{SF} = 0.015/(3.5/0.6) = 0.0026$. Adopting $k_{Ia} = 0.003 M_{\odot}^{-1}$ and an Fe production of 0.6 M_{\odot} per SNIa event, the Fe productivity from SNIa's is of 0.0018, which accounts for $\sim 70\%$ of the Fe content in galaxy clusters; the remaining 30% would be produced by CC SNe.

Fig. 11 shows that the models with a flat distribution of the separations (dotted lines) tend to over predict the rate in Ellipticals, in both DD CLOSE and DD WIDE cases. This problem is lessened for the Solomonian mixture, due to the dramatic drop of the SD channel at long delay times. However, when considering the merged E+S0 class, the DD CLOSE model with a flat distribution of A becomes compatible with the data. It is then very important to derive a robust measurement of the SN Ia rate separately for the two morphological types: in early type galaxies, a difference in average age of ~ 2 Gyr has a strong effect on the SN Ia rate per unit mass, if a sizable contribution from the SD channel exists. The fact that the rate in SNU's in S0 galaxies appears so much higher than in Es favours this interpretation, although the statistics is still too poor to draw such conclusion. In this respect, the SD model appears to best represent the data. However, the green lines in Fig. 11 are obtained with a choice for the accretion efficiency and distribution of the mass ratios which maximize the fraction of systems with long delay times; any other choice would lead to an underproduction of SNIa events in E galaxies.

Considering now the rates in late type galaxies, all models are consistent with the data within the very large error bar, although the predicted rates are lower than the average observed values. The parameter $\tau_{n,x}$ which has some impact on the fraction of events at short delay times (see Sect. 3.2) does not appear to play a role in the fit (e.g. DDC1 vs DDC3). In a star bursting regime the SN Ia rate gets substantially increased (crosses), especially when the DTD is particularly skewed towards the short delay times. As mentioned above, the galaxy modelling presented here does not reproduce satisfactorily the colors of Irregulars with either tested shapes for the SF rate. A more precise assessment of the recent SF in galaxies of the latest types is crucial to derive information on the DTD from their observed SN Ia rates.

As a general conclusion, the trend of the SN Ia rate as function of the morphological type suggests that the DTD ought to be significantly decreasing at the very long delay times. This disfavors flat distributions of the separations in the case of DD progenitors. Provided that, the fit obtained with the mixed models is not particularly better than that with single channel models.

4.2 Rates as function of specific star formation

Sullivan et al. (2006) measured the SN Ia rate per unit mass as a function of the current star formation rate per unit mass for the Supernova Legacy Survey (SNLS) galaxy sample (Sullivan et al. 2005). The correlation is based on 124 SN Ia at redshifts between 0.2 and 0.75. It is worth recalling that in this work the galaxy masses were determined via spectral energy distribution (SED) fitting to PÉGASE 2.2 models (Fioc & Rocca-Volmerange 1997) with Kroupa (2001) IMF, and that the SSFR is measured as the ratio between the mean SF rate over the last 0.5 Gyr and the current stellar mass of the galaxy, resulting from the SED fitting.

Black dots in Fig. 12 show the observed relation for the star forming galaxies in Sullivan et al. (2006); coloured dots and lines are models constructed for a wide variety of SF histories, so as to illustrate the impact on the theoretical relation of the adopted SF law, and of the galaxy age. Given their redshift range, the SN Ia host galaxies should have current ages between ~ 7 and 11 Gyr, or younger. Technically, the theoretical specific SN Ia and SF rates are computed as:

$$\frac{\dot{n}_{\text{Ia}}(t)}{M_{\text{SF}}} = k_{\text{Ia}} \int_0^t \psi(t-\tau) f_{\text{Ia}}(\tau) d\tau \quad (7)$$

$$\frac{\dot{M}}{M_{\text{SF}}} = 2 \cdot 10^{-9} \frac{\int_{t-0.5}^t \psi(t) dt}{\int_0^t \psi(t) dt} \quad (8)$$

where t is the current age and M_{SF} is the mass transformed into stars up to now. Because of the mass return from dying stars, M_{SF} is always higher than the current stellar mass in a galaxy, by a factor of $\sim 1.6, 1.3$ for old and young stellar populations, respectively. These values hold for a bottom light IMF, such as Kroupa's, and for galaxy ages older than ~ 1 Gyr. Therefore, accounting for the mass return corresponds to shifting the models up and right by $\sim 0.1 - 0.2$ dex, the correction being however different for each model, since it depends on age and SF history. Given the differences in the galaxy modelling between Sullivan et al. (2006) and this paper, rather than correcting each model, the data points (read off Fig. 3 in Pritchett, Howell & Sullivan 2008) have been shifted by a variable amount (see caption). The applied correction is meant to represent the average ratio of the current stellar mass to the total mass gone into stars in the five bins. As usual, the productivity k_{Ia} in Eq. (7) is a free parameter; however the models in Fig. 12 have been all computed with $k_{\text{Ia}} = 10^{-2.8} M_{\odot}^{-1}$ irrespective of the DTD, a value which turns out to describe very well the SN Ia rate in the bin at $\text{SSFR} = 10^{-10} \text{ yrs}^{-1}$. A refined fit of the SN Ia productivity seems unworthy, since the models and the data are not completely compatible as just discussed, and since the SF history of the galaxies is not well constrained.

The slope of the theoretical correlation between the rate per unit mass and the SSFR appears virtually insensitive to the assumed SF history, for star forming galaxies, as already pointed out by Pritchett et al. (2008). The models overlap each other along a locus which is well described by a power law along which the younger the galaxy (either because of its current or its average age), the higher its SSFR, and its SN Ia rate per unit mass. The exponent of the power law is sensitive to the model DTD; for the models plotted in Fig. 12 it ranges from 0.6 (SD model) to 0.8 (Segregated mixture with DDC1 model). In addition, the theoretical relation is found systematically steeper for the Segregated mixtures compared to Solomonian mixtures or Single channel models.

In general, all DTDs yield an acceptable representation of the data. Taken at face value, the observed correlation seems to favour models with a moderate power at the early delay times, as the SD model, or the Solomonian mixtures. The Segregated mixtures tend to predict a too high SN Ia rate in star bursting galaxies at given SSFR value, but no strong conclusion can be drawn from this comparison. Sullivan et al. (2006) also determine the SN Ia rate per unit mass in *passive* galaxies (from SNLS data), which turns out very close to the rate measured for galaxies in the bin at $\text{SSFR} = 10^{-11} M_{\odot}/\text{yr}$. This point is not plotted on Fig. 12, where, instead, I show the location of two models for old stellar populations (see caption), in which most of the stellar mass has been made at high redshift. These models have virtually null current specific SF rate and yet their current SN Ia rate is relatively high due to the late delay times component of the DTD. This interpretation differs from what concluded in Pritchett et al. (2008) mainly because of the different rendition of the SF history in passive galaxies. Adopting Eq. 5 with a short τ_{SF} , the SSFR quickly drops as the time from the beginning of star formation increases, so that negligible SSFR are obtained when the SNIa rate is still relatively high because of the *tardy* component. For example, a model with $\tau_{\text{SF}} = 2$ Gyr, at an age of 10 Gyr has a SSFR of $1.8 \cdot 10^{-14} M_{\odot}/\text{yr}$ and an average age of 7.5 Gyr. With this star formation history, the SD DTD plotted in Fig. 12 predicts a SNIa rate of $4.7 \cdot 10^{-14} (M_{\odot}/\text{yr})^{-1}$, matching the rate in passive galaxies determined by Sullivan et al. (2006). However, as noticed in the

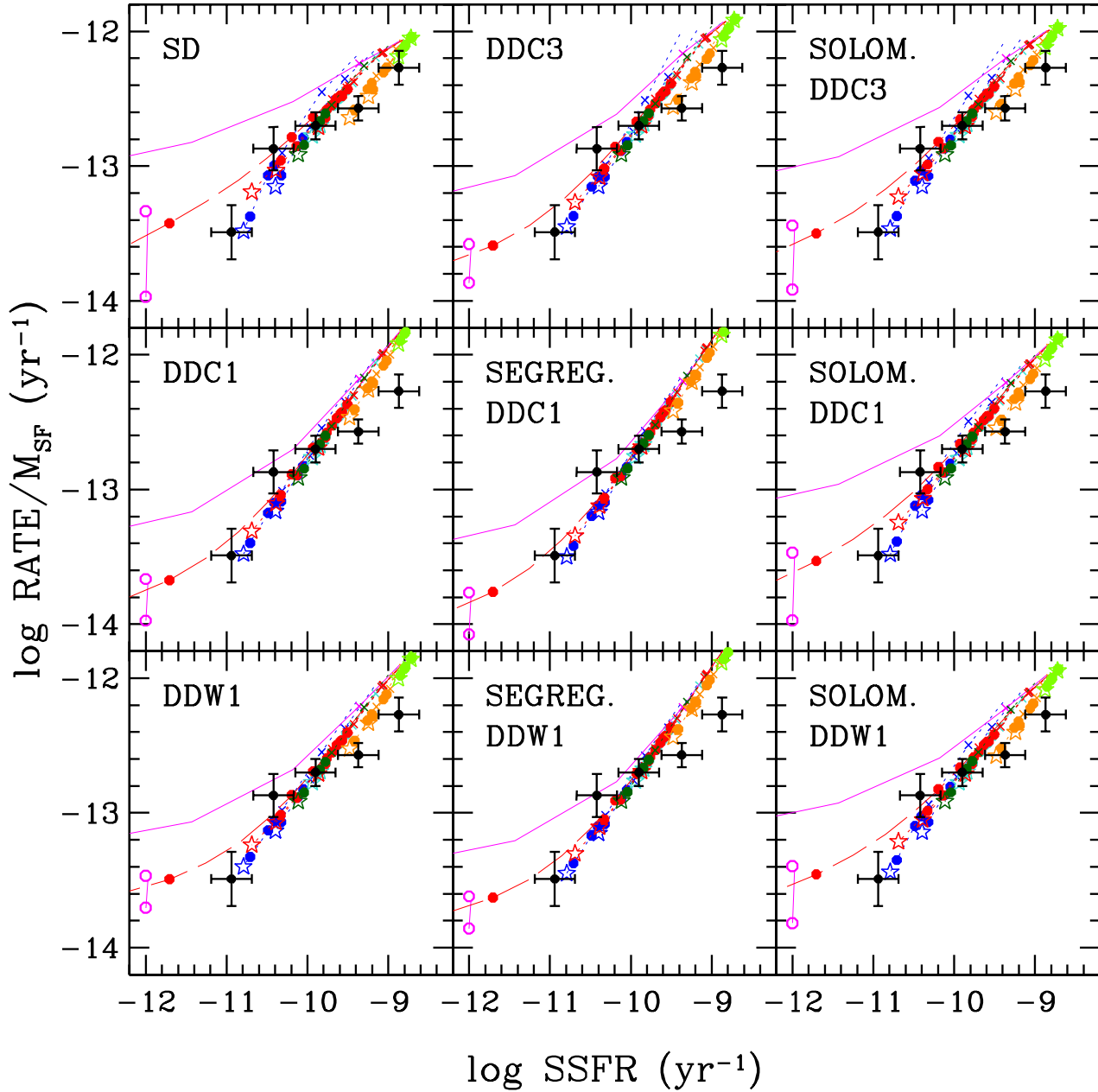


Figure 12. Correlation between the SN Ia rate and the SF rate both normalised to the total mass transformed into star. The data (black dots) are from Sullivan et al. (2006) shifted down and left to account for the mass return, by (0.12,0.12,0.15,0.17,0.19) dex for the 5 bins from right to left. The models (coloured lines and dots) assume different DTDs as labelled in each panel (see caption to Fig.11 for the meaning of the acronyms). The colours encode the kind of SF history: (i) currently bursting, with a ratio of current to past SF rate of 500, 50 (light green), 10, 5 (orange); (ii) power laws with exponent -0.9 and -0.5 (blue), 0.5 and 0.9 (cyan); (iii) ψ given by Eq. (5) with $\tau_{SF}=1$ (magenta), 3, 5, 6 and 20 Gyr (red). The lines show the models as they age from 1 to 13 Gyr; crosses show the location at 2 and 5 Gyr, full dots at 6, 7 and 11 Gyr, the stars mark the position at 13 Gyr. The two open dots show the rates of the model with ψ given by Eq. (5) and $\tau_{SF}=1$ Gyr at an age of 7 (upper) and 11 (lower) Gyr. Notice that the SSFR of these models is much lower than 10^{-12} yr^{-1} , and virtually null.

previous section, such SD model assumes a 100 % accretion of the envelope of the secondary onto the CO WD, and a flat distribution of q , so that the rate at late epochs is enhanced. For this reason, DD models, and/or Solomonic mixtures could be more plausible.

5 SUMMARY AND DISCUSSION

This paper presents the theoretical expectations for SN Ia progenitors focusing on two questions: the shape of the distribution of the delay times and the possible diversity of SN Ia progenitors of events at different delay times. These two issues impact on the cosmolog-

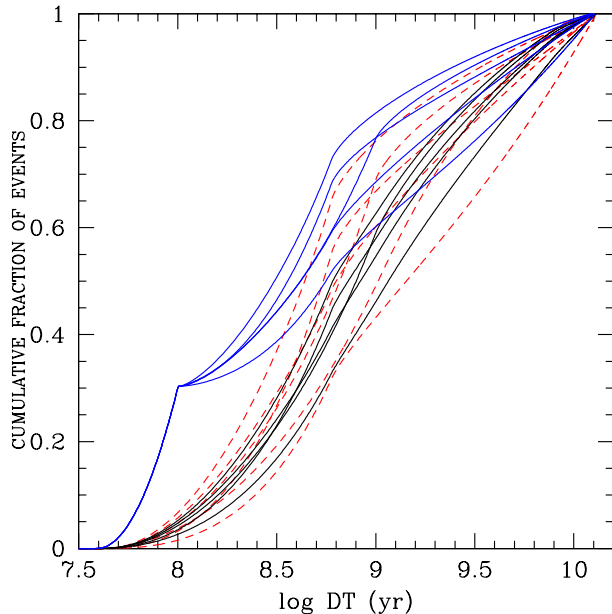


Figure 13. Cumulative fraction of events as the delay time grows for the DTDs used in Fig. 11. Dashed red, solid black and solid blue lines refer respectively to single channel, Solomonic mixtures and Segregated mixtures.

ical use of SN Ia’s as distance indicators because they may entail a systematic diversity between events at low and high redshift, where the progenitors are younger and more massive. As in Paper I, the approach refrains from describing the evolution of individual systems, rather concentrating on the clock of the explosion and on a few parameters singled out as crucial for the two issues. In particular, different from BPS renditions, the mass exchange phases during the binary evolution are not followed, and their result in promoting or not the final event is considered as an equally plausible option. The dependence of the likelihood of the SN Ia event on the initial binary separation is also neglected, having assumed that (i) there is a range of separations suitable for the realisation of the SN Ia, and that (ii) this range does not depend on the other binary parameters (m_1 and m_2). While strictly speaking the latter assumption is untrue (see discussion at the beginning of Section 2.3), the comparison of the analytic DTDs with the results of BPS simulations seem to indicate that the crucial parameters are indeed the masses of the components.

I have illustrated the main features of the analytic DTD for the single and the double degenerate evolutionary channels, concentrating on Chandrasekhar exploders, since Sub-Chandra models are currently disfavoured. Nevertheless, it is worth pointing out that Sub-Chandra events could be important especially to account for SN Ia’s in old stellar populations. Actually these events are an embarrassment, since they are much easier realised than Chandra explosions, yet there are no established observational counterparts. Crucial parameters for shaping the SD DTD are the limits on the primary and on the secondary mass, and the efficiency of accretion onto the CO WD. The DTD is populated only within delay times comprised between the MS lifetime of the most and least massive secondary in the progenitor’s system; a lower accretion efficiency results into a steepening of the DTD at late epochs. If only half of the envelope of the secondary is used for the mass growth of the CO WD, the DTD drops by three order of magnitudes between 1 and 10 Gyr, making the rate in old stellar systems negligibly small.

For both flavours of DD models (CLOSE and WIDE), the major parameters are the minimum mass of the secondary in successful systems and the slope of the distribution of the separations of the DD systems at birth. Additional parameters are the minimum values for the delays τ_n and τ_{GW} , the former being directly connected to the maximum value of m_2 in successful systems. The comparison of the analytic DTDs with results in the literature shows a very good agreement with BPS renditions for the DD CLOSE channel (renditions for the DD WIDE channel are lacking in the literature). Less favourable is the comparison for the SD channel, for which the BPS results yield a large variety of DTD shapes. Clearly, in the simulations, the efficiency with which this channel produces SN Ia events is very sensitive to the criteria adopted to describe the mass exchange phases and the fate of the accreting WDs.

5.1 Prompt and tardy components

In principle, all channels accommodate *prompt* and *tardy* events, but the DTD is very continuous so that this distinction appears artificial. As illustrated in Fig. 13, for the single channel DTDs, the cumulative fraction of explosions smoothly increases with the delay time, so that the fraction of *prompt* events depends on the definition of the timescale over which the events are considered as such. As shown in Figs 11 and 12 these DTDs, with no strong discontinuity, do account well for the observed trends of the SN Ia rates with the parent stellar population.

Motivated by recent observations which suggest that both SD and DD explosions may be realised in nature, I have constructed mixed models under two extreme assumptions: the *Solomonic* option, in which the two channels contribute the same fraction of events within a Hubble time, and the *Segregated* mix, in which the SD and DD channels feed distinct ranges of delay times. Since the SD model has difficulties to account for late epoch explosions, I assumed that it provides a very *prompt* component of the DTD. This composition allows one to introduce a sharp discontinuity when the channel producing the events changes; the position in delay time of this discontinuity has been (arbitrarily) fixed at 0.1 Gyr to mimic the DTD proposed by Mannucci et al. (2006). In the attempt of constraining the DTDs, either single channel or mixed models, I have considered the observed correlations between (i) the SN Ia rate per unit luminosity and the parent galaxy type (GC09), and (ii) the SN Ia rate per unit mass and the specific SF rate of the parent galaxy (Sullivan et al. 2006). Theoretical expectations have been computed with a population synthesis technique, adopting a variety of SF histories for the galaxies. To construct the first of the two correlations, the galaxies’ ($U - V$) and ($B - K$) colours have been used to constrain the SF history; correlation (ii) turns out largely independent of the adopted shape for the SF, as found by Pritchett et al. (2008). The observed correlation between the SN Ia rate per unit luminosity and the parent galaxy morphological type appears to require a substantial depletion of the DTD at late delay times. This holds especially for the rate measured in SNU’s and derives from the drop of the rate going from S0 to E galaxies, which is not detectable when the two classes are merged together. In fact, the colours of S0s and Es indicate that the former are slightly younger, although both galaxy types are dominated by old stellar populations. S0s and Es, then, probe the DTD at very late delay times, where, e.g., the SD model predicts a considerable drop. The steepening of the rate going from S0 to Es measured in GC09 supports DTDs with a steep decline at late delays, as the SD channel, or Solomonic mixtures. The DD channel and the Segregated mix could also meet this constraint, provided that the distribution of the separations is skewed at

the short end. This interpretation needs to be confirmed with larger galaxy samples and more SN Ia events.

The correlation between the SN Ia rate and the galaxy type does not provide a robust constraint on the shape of the DTD at short delay times, because the SF history in the latest galaxies is not known with sufficient accuracy, and, admittedly, the colours of Irregulars are not well reproduced by the populations synthesis presented here. The theoretical rates are found consistent with the data for Irregulars and Sc galaxies even with the relatively low fraction of *prompt* events of the SD model, but a better understanding of the recent and past SF history in these galaxies is needed to derive robust conclusions.

The correlation between the SN Ia rate per unit mass and the SSFR is compatible with the models for most of the explored DTDs, although the rates in the star bursting galaxies indicate that the DTD should not be too skewed at the short delay times, thus disfavouring very steep DD CLOSE models and Segregated mixtures. Models computed with the SD DTD yield a very nice description of the correlation for the star forming galaxies; the rate in passive galaxies may also be well reproduced with this DTD if their inhabiting stellar populations have a (small) age spread: e.g., one model galaxy having formed $\sim 80\%$ of its current mass within the first 1.7 Gyr, at an age of 9 Gyr has a SN Ia rate⁵ of $\approx 4.2 \cdot 10^{-14} (M_{\odot}\text{yr})^{-1}$ very close to what determined for the passive galaxies in Sullivan et al. (2006) ($\approx 5 \cdot 10^{-14} (M_{\odot}\text{yr})^{-1}$). However, this estimate assumes that all of the envelope of the secondary is accreted by the CO WD companion, which looks contrived.

5.2 SN Ia productivity

The fit of the observed relations yields a value for the productivity k_{Ia} , i.e. the number of SN Ia's produced by a unit mass stellar population over the whole range of delay times. In general k_{Ia} depends on the IMF, DTD and SF history assumed to model the galaxies, but the dependence on the DTD is small for systems in which the SF rate varies little over the whole range of ages, and actually vanishes for a constant SF rate (see Paper I). Therefore, in this paper, the value of k_{Ia} is derived by matching the level of the SN Ia rate in galaxies of intermediate type (Sa-Sb). Assuming a bottom light IMF (Salpeter flattened below $0.5 M_{\odot}$), from the rates in SNU's (SNUK's) in GC09 I find $k_{\text{Ia}} \approx 3.3(2.8) \times 10^{-3} M_{\odot}^{-1}$, with a 50 % total variation for all the DTDs plotted in Fig. 11 (single and mixed channels). This value requires that $\approx 8\%$ of all stars with mass between 2.5 and $8 M_{\odot}$ produce a SN Ia event. For the Segregated mixture, 30 % of the progenitors are assumed to come from systems with m_2 between 5 and $8 M_{\odot}$: this corresponds to a likelihood of the SN Ia event of $\sim 10\%$ from the more massive progenitors, and of $\sim 4\%$ for stars with mass between 5 and $2.5 M_{\odot}$.

It is instructive to compare the SN Ia to the core collapse (CC) SNe productivity (k_{CC}) for the same IMF. The number of CC events per unit mass from a stellar generation depends on mass limits of the progenitors; assuming an upper limit of $40 M_{\odot}$, it amounts to 6.5 (9) events every $1000 M_{\odot}$ for a lower limit of 10 (8) M_{\odot} , having adopted a Salpeter flattened IMF. Thus, each stellar generation is expected to produce ~ 2 -3 CC SNe per SN Ia; the events, though, occur at different delay times: all the CC explosions take place soon after the star formation episode, while the SN Ia events are diluted over the whole Hubble time, with only the *prompt* component exploding early. For the Segregated mixture considered here, a 1000

M_{\odot} stellar populations provides ≈ 1 (*prompt*) SN Ia within 0.1 Gyr from birth; the same stellar population provides ~ 7 CC SNe within 30 Myr from birth. Therefore, a sample of elliptical galaxies supposed to have experienced a starburst within the last 0.1 Gyr should yield 7 CC to 1 Ia *prompt* events; thus the excess of 7 SN Ia's in radio loud ellipticals noticed by Della Valle et al. (2005) should be accompanied by ~ 50 CC events in the same galaxy sample, while none was observed. This observational result would require a detection efficiency of CC events ~ 50 times lower than that of Ia events, which is very hard to understand. The problem of the *missing* CC SNe in radio loud Ellipticals becomes worse if the CC productivity is higher, as implied, e.g., by a lower limit of $8 M_{\odot}$ for their progenitors. It is worth noticing that although dust obscuration may preferentially hide CC SNe, since they explode soon after the onset of SF, in late type spirals 2.5 CC events are detected every 1 SNIa (Cappellaro, Botticella & Greggio 2007), which shows that dust does not have that dramatic effect at least in this kind of galaxies.

The productivity k_{Ia} can also be determined by fitting the rates from Sullivan et al. (2006). Matching the SN Ia rate in galaxies with $\text{SSFR} = 10^{-10} (M_{\odot}\text{yr})^{-1}$ requires $k_{\text{Ia}} \approx 1.6 \times 10^{-3} M_{\odot}^{-1}$, which is ~ 2 times lower than what estimated from the rates per unit luminosity. Notice that with this lower productivity, the problem of the *missing* CC events in radio loud Ellipticals worsens. The discrepancy between the productivities estimated from the two kinds of correlations may be due to the different astrophysical ingredients for the stellar population models adopted here and in Sullivan et al. (2006): the IMF, the SF history (i.e. age and metallicity distribution) of the galaxies, the stellar tracks to describe their light. In fact, in order to obtain the observational SN Ia rates and SSFR, assumptions are necessary for all of these ingredients. In addition, the estimates for k_{Ia} derived here represent zero point determinations, rather than accurate fits to the data, and the true distance between the best fitting k_{Ia} values from the two correlations could be smaller than what quoted above. All in all, the results on the productivity of SN Ia's from matching the observed rates are rather encouraging, though there seems to be a systematic difference between the values derived from the two data sets, with the rate per unit luminosity requiring a factor of ~ 2 higher productivity. Whether this is a robust conclusion or not can be established only with complete consistency of assumptions in modelling and observational estimates.

5.3 Diversity of SN Ia events

The astrophysical parameter responsible for the diversity of ^{56}Ni production, and then of SN Ia light curves, has not been identified yet. A number of possibilities have been proposed in the literature, some of which related to the progenitor, like metallicity, age, ignition density, others more related to the physical phenomena taking place during the explosion (Hoeftlich & Khokhlov 1996; Kasen, Roepke & Woosley 2009). From an empirical point of view, the most conspicuous evidence concerns the correlation between the SN Ia light curve properties and the (average) age of the parent stellar population (Gallagher et al. 2008; Howell et al. 2009), metallicity playing, in case, a secondary role. This suggests the possibility that the diversity of SN Ia's is strongly related to their delay time.

According to stellar evolution one expects a trend for the average mass and temperature of the WD progenitor with delay time, but with a substantial spread. For the SD model, the average mass of the CO WD at the start of accretion first decreases, reaches a minimum, but then increases again, since at the late delay times only

⁵ This estimate assumes $k_{\text{Ia}} = 10^{-2.8} M_{\odot}^{-1}$ and 37 % a mass return.

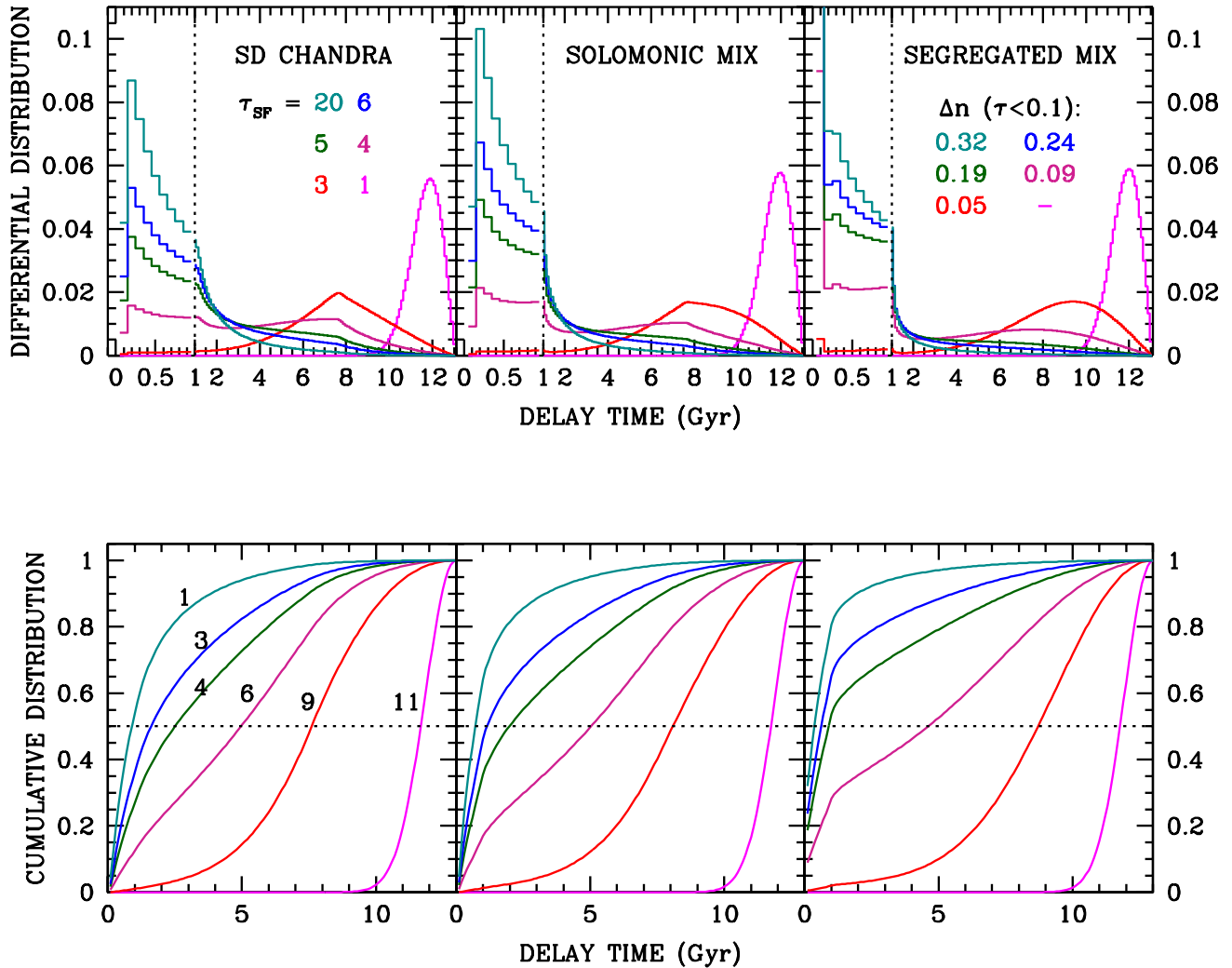


Figure 14. Differential (upper panels) and cumulative (lower panels) distributions of the delay times of events exploding in 13 Gyr old galaxies. Different panels show the results for different DTDs, as labelled in the upper figure; the mixed models assume a DD component of the CLOSE variety with $\tau_{n,x}=1$ and $\beta_g=-0.975$ (DDC3). The colour encodes the SF history, given by Eq.5 with different values of τ_{SF} , labelled in the upper left panel. The values 20, 6, 5, 4, 3, and 1 Gyr produce model galaxies with colours akin to Irregulars, Sc, Sb, Sa, S0 and E, respectively. For the Segregated mixture, the fraction of events with delay time shorter than 0.1 Gyr obtained with the different SF histories is labelled in the upper right panel. The curves in the lower left panel are labelled with the (B luminosity weighted) average age of the galaxy model. Notice that the delay time scale in the upper panels has been expanded between 0 and 1 Gyr for better readability of the figure.

massive CO WDs are able to grow up to the Chandrasekhar limit. The range encompassed by the mass of the CO WD is maximum at $\tau \sim 1$ Gyr, but becomes narrower at late delays. For the DD WIDE channel, the total mass of the successful DD system is expected to vary between 1.4 and 2.4 M_{\odot} (almost) irrespective of the delay time, since for each combination of m_1 and m_2 , small and wide separations should be realised, thereby providing events with any gravitational wave radiation delay. For the DD CLOSE channel, instead, we expect a trend of decreasing average M_{DD} as τ increases, because the more massive the progenitors, the smaller the separation of the DD system, and then the shorter the time needed to merge. The time between the formation of the CO WD and its final explosion is an increasing function of the delay time. Thus, for the

DD CLOSE channel, the progenitors of events at short delay times are massive and hot (when accretion starts), while at long delay times they are of low mass and cool. According to Lesaffre et al. (2006) models these two parameters could induce compensating trends on the ignition density, and the ^{56}Ni mass synthesised in the explosion may not show big variations over the total range of delay times. It is worth pointing out, however, that the models explore a range of relatively short cooling times (up to 1 Gyr), while the WD progenitors of SN Ia's in early type galaxies have been cooling for many Gys. The outcome of the explosion of CO WDs which start accreting when their structure is so highly degenerate needs to be investigated.

Regardless the key astrophysical variable which causes the di-

versity of SN Ia light curves (whether ignition conditions, metallicity, evolutionary channel leading to the explosion), if this variable scales systematically with the delay time one expects a trend of the typical properties of SN Ia light curve with the age distribution in the parent stellar population. The observed correlation will depend on the SF history of the galaxies and on the DTD: the younger the stellar populations and/or the higher the fraction of short delay times, the higher the likelihood that a detected SN Ia event has a short τ .

As an illustrative example, Fig. 14 shows the distribution of the delay times of events occurring in galaxies with 13 Gyr of age, having experienced different SF histories. The differential distributions are computed as:

$$\Delta n = \frac{\int_{\tau}^{\tau+\Delta\tau} \psi(13-\tau) f_{\text{Ia}}(\tau) d\tau}{\int_0^{13} \psi(13-\tau) f_{\text{Ia}}(\tau) d\tau} \quad (9)$$

and represent the probability that a SN Ia detected in a galaxy of a certain type has a given delay time. It appears that in the late galaxy types most of the events cover a range of delay times up to about 1-2 Gyr: as shown in Sect. 3 this is wide enough to encompass the whole range of masses of the CO WDs. Only in the case of strongly star bursting galaxies the majority of events may come from a truly *prompt* component, i.e. the most massive and hottest CO WDs. Even for the Segregated mixture in combination with the model for Irregular galaxies, more than 40 % of the SN Ia's should have a delay time in excess of 0.5 Gyr. In Sa galaxies all the delay times have about the same probability of being sampled, and the distribution remains wide also in S0 galaxies, though mostly confined at $\tau \gtrsim 5$ Gyr; in Ellipticals, instead, we expect to sample only the latest delay times. Therefore, if diversity were related to the delay time, SN Ia's in Es should be rather uniform, while in later galaxy types we should detect a large variety of light curve properties, as suggested by the data. Notice that in the DD WIDE channel the mass range of the successful DD systems is not likely to become narrower at late delays: for this model, if diversity was connected to M_{DD} , a wide range of light curve properties should be observed also in the earliest galaxy types.

Uniformity of events in old galaxies is supported in Howell et al. (2009), but it is difficult to understand quantitatively the result that galaxies with a light averaged age in excess of 3 Gyr host only faint supernovae (technically with a low ejected ^{56}Ni mass). The curves plotted in the bottom left panel of Fig. 14 are labelled with the B-light averaged age of each galaxy model. Only Irregulars and Sc galaxies appear younger than 3 Gyr, while Sb's and Sa's have an average age of several Gyrs. In these galaxies the distribution of the delay times of their hosted SN Ia's is predicted rather broad, which would imply a broad range of photometric properties, irrespective of the specific DTD model. Therefore, it is difficult to reconcile the notion that delay time is primarily responsible for diversity of SN Ia events with Howell et al. (2009) result.

6 CONCLUSIONS

According to expectations of stellar evolution in close binaries the DTD is a continuous distribution, skewed at the short delay times, but with no real justification for a separate *prompt* component. Mixed models may implement this concept, e.g. considering that the two channels (SD and DD) feed distinct ranges of delay times. However, there's no clear theoretical reason why it should be so,

and the observed correlations between the specific rates and the parent galaxy properties do not appear to require it.

Indeed, the observed correlations do not favour mixed over single channel models. The indication of the two channels being active comes from the data of individual explosions. More data are needed to establish whether the SD explosions are favoured at short delay times, i.e. in young stellar populations, which could support the Segregated mixture models presented here.

The correlation between the SN Ia rate per unit B-luminosity and the parent galaxy type suggests a steep drop of the DTD at late epochs, consistent with the SD or DD models with a distribution of separations depleted of wide systems. The correlation between the SN Ia rate per unit mass and the specific SF rate is (broadly) consistent with this kind of models, and seems to require a relatively small fraction of *prompt* events. However, in order to constrain the fraction of short delay times in the DTD we need a more accurate description of the SF history in galaxies with high SSFR and of the latest morphological types.

The observed rates allow us to evaluate the SN Ia productivity k_{Ia} , which appears to be in the range $(1.6 - 3.3) 10^{-3} M_{\odot}^{-1}$. Although it is reassuring that the different data sets yield values which agree within a factor of ~ 2 , there may be a systematic difference between the productivity evaluated from the rates per unit luminosity and per unit SSFR. On the other hand, the ingredients adopted for the galaxies' modelling to fit the two correlations are not exactly the same. Therefore the discrepancy on the SN Ia productivity may just reflect a theoretical uncertainty.

Concerning the diversity of SN Ia light curves, we expect a wide range for the mass of the CO WDs at the start of the accretion phase in most galaxy types; only in the older stellar populations the properties of the progenitors should be more uniform. For mixed models, in both the Solomonic and Segregated flavours, late type galaxies should host SD and DD events with comparable probability, while in early type galaxies most, if not all, SN Ia should come from DD progenitors. Only in very young stellar populations, with very high specific SF, the SD events are likely to prevail. Current data on the correlation between the light curve properties and the host galaxy seem to yield contradictory indications, possibly because of the use of different parameters to characterise the SN Ia light curve and the properties of the host galaxy. Progress requires big samples of events, as well as more accurate knowledge of the age distribution in SN Ia hosts; on the theoretical side more models are also needed, in particular exploring the fate of an accreting CO WD which has been cooling for several Gyrs, hence starting from highly degenerate conditions.

A broader diversity of progenitor's properties is expected in local SN Ia samples compared to high redshift ones, since the former encompass all possible delay times, while the latter necessarily lack events with delay times longer than the corresponding age of the universe. Nevertheless, a fair fraction of explosions in nearby star forming galaxies (spirals and irregulars) should have a short delay time, e.g. shorter than 1 Gyr. Therefore the empirical *standardisation* of the light curve obtained from the SN Ia's in nearby star forming galaxies should be applicable also to high redshift events, thus supporting SN Ia's as viable standard candles all the way to cosmological distances.

ACKNOWLEDGMENTS

I am indebted to Alvio Renzini for helpful discussions and comments, and for careful reading of the manuscript. I also thank En-

rico Cappellaro for discussions and for checking on the discrepancy between the SN Ia rate in early type galaxies determined by Mannucci et al. (2005) and by GC09. Finally, I thank the anonymous referee for productive comments.

REFERENCES

- Abt H.A., 1983, *ARA&A*, 21, 343
- Altavilla G. et al., 2004, *MNRAS*, 349, 1344
- Arnett D., 1982, *ApJ*, 253, 785
- Belczynski K., Bulik T., Ruiter A.J., 2005, *ApJ*, 629, 915
- Bessell M.S., 1990, *Publ. Astron. Soc. Pac.*, 102, 1181
- Blanc G., Greggio L., 2008, *New Astron.*, 13, 606
- Cappellaro E., Evans R., Turatto M., 1999, *A&A*, 351, 459
- Cappellaro E., Botticella M.T., Greggio L., 2007, in Immler S., Weiler K., McCray R., eds, *AIP Conf. Proc.* 937, *Supernova 1987A:20 Years After: Supernovae and Gamma-Ray Bursters*. Am. Inst. Phys., New York, p. 198
- Ciotti L., D'Ercole A., Renzini A., Pellegrini S., 1991, *ApJ*, 376, 380
- Della Valle M., Panagia N., Padovani P., Cappellaro E., Mannucci F., Turatto M., 2005, *ApJ*, 629, 750
- de Vaucouleurs G., de Vaucouleurs A., Corwin H.G., Buta R.J., Paturel G., Fouque P., 1991. *Third Reference Catalogue of Bright Galaxies*. Springer-Verlag, New York
- Di Stefano R., Primini F.A., Liu J., Kong A., Patel B., 2009, preprint (arXiv:0909.2046)
- Ellis, R.S. et al., 2008, *ApJ*, 674, 51
- Fioc M., Rocca-Volmerange B., 1997, *A&A*, 326, 950
- Gallagher J.S., Garnavich P.M., Caldwell N., Kirshner R.P., Jha S.W., Li W., Ganeshalingam M., Filippenko A.V., 2008, *ApJ*, 685, 752
- Gavazzi G., Bonfanti C., Sanvito G., Boselli A., Scodreggio M., 2002, *ApJ*, 576, 135
- Greggio L., 1996, in Kunth D., Guiderdoni B., Heydari-Malayeri M., Thuan T.X., eds. *The Interplay Between Massive Star Formation, the ISM, and Galaxy Evolution*. Edition Frontières, Gif-sur-Yvette, p. 98
- Greggio L., 2005, *A&A*, 441, 1055 (Paper I)
- Greggio L., Cappellaro E., 2009, in Antonelli L.A., Brocato E., Limongi M., Menci N., Raimondo G., Tornambé A., eds, *AIP Conf. Proc.* 1111. *Probing Stellar Populations Out to the Distant Universe*. Am. Inst. Phys., New York, p.477 (GC09)
- Greggio L., Renzini A., 1983, *A&A*, 118, 217
- Greggio L., Renzini A., Daddi E., 2008, *MNRAS*, 388, 829
- Hachisu I., Kato M., Nomoto K., 1996, *ApJ*, 470, L100
- Hachisu I., Kato M., Luna G.J.M., 2007, *ApJ*, 659, L153
- Hachisu I., Kato M., Nomoto K., 2008, *ApJ*, 683, L127
- Han Z., Podsiadlowski Ph., 2004, *MNRAS*, 350, 1301
- Hicken M. et al., 2009, *ApJ*, 700, 331
- Hillebrandt W., Niemeyer J.C., 2000, *ARA&A*, 38, 191
- Hoeflich P., Khokhlov A., 1996, *ApJ*, 457, 500
- Hoeflich P., Khokhlov A., Wheeler J.C., Phillips M.M., Suntzeff N.B., Hamuy M., 1996, *ApJ*, 472, L81
- Howell D.A. et al., 2006, *Nature*, 443, 308
- Howell D.A. et al., 2009, *ApJ*, 691, 661
- Iben I.Jr, 1991, *ApJS*, 76, 555
- Iben I.Jr, Tutukov A.V., 1987, *ApJ*, 313, 727
- Iben I.Jr, Tutukov A.V., 1994, *ApJ*, 431, 264
- Lesaffre P., Han Z., Tout C.A., Podsiadlowski Ph., Martin R.G., 2006, *MNRAS*, 368, 187
- Kalirai J.S., Hansen B.M.S., Kelson D.D., Reitzel D.B., Rich R.M., Richer H.B., 2008, *ApJ*, 676, 594
- Kasen D., 2010, *ApJ*, 708, 1025
- Kasen D., Roepke F.K., Woosley S.E., 2009, *Nature*, 460, 869
- Kenyon S.J., Livio M., Mikolajewska J., Tout C.A., 1993, *ApJ*, 407, L81
- Kouwenhoven M.B.N., Brown A.G.A., Portegies Zwart S.F., Kaper L., 2007, *A&A*, 474, 77
- Kroupa P., 2001, *MNRAS*, 322, 231
- Maíz Appellániz J., 2006, *AJ*, 131, 1184
- Mannucci F., Della Valle M., Panagia N., Cappellaro E., Cresci G., Maiolino R., Petrosian A., Turatto M., 2005, *A&A*, 433, 807
- Mannucci F., Della Valle M., Panagia N., 2006, *MNRAS*, 370, 773
- Matteucci M.F., Greggio L., 1986, *A&A*, 154, 279
- Matteucci M.F., Panagia N., Pipino A., Mannucci F., Recchi S., Della Valle M., 2006, *MNRAS*, 372, 265
- Marigo P., Girardi L., Bressan A., Groenewegen M.A.T., Silva L., Granato G.L., 2008, *A&A*, 482, 883
- Mazzali P.A., Nomoto K., Cappellaro E., Nakamura T., Umeda H., Iwamoto K., 2001, *ApJ*, 547, 988
- Meng X., Chen X., Han Z., 2009, *MNRAS*, 395, 2103
- Mereghetti S., Tiengo A., Esposito P., La Palombara N., Israel G.L., Stella L., 2009, *Sci*, 325, p. 1222
- Munari U., Renzini A., 1992, *ApJ*, 397, L87
- Napiwotzki R., et al., 2005, in Koester D., Moehler S, eds, *ASP Conf. Series* 334. *14th European Workshop on White Dwarfs*. Astron. Soc. Pac., San Francisco, p.375
- Neill J.D. et al., 2009, *ApJ*, 707, 1449
- Nelemans G., Verbunt F., Yungelson L.R., Portegies-Zwart S.F., 2000, *A&A*, 360, 1011
- Nobili S., Goobar A., 2008, *A&A*, 487, 19
- Nomoto K., Iben I.Jr, 1985, *ApJ*, 297, 531
- Nomoto K., Kamiya Y., Nakasato N., Hachisu I., Kato M., 2009, in Antonelli L.A., Brocato E., Limongi M., Menci N., Raimondo G., Tornambé A., eds, *AIP Conf. Proc.* 1111. *Probing Stellar Populations Out to the Distant Universe*. Am. Inst. Phys., New York, p.267
- Nugent P., Baron E., Branch D., Fisher A., Hauschildt P.H., 1997, *ApJ*, 485, 812
- Oemler A., Tinsley B.M., 1979, *AJ*, 84, 985
- Parthasarathy M., Branch D., Jeffery D.J., Baron E., 2007, *New Astron. Rev.*, 51, 524
- Patat F. et al., 1997, *Sci.*, 317, 924
- Perlmutter S. et al., 1997, *ApJ*, 483, 565
- Perlmutter S. et al., 1999, *ApJ*, 517, 565
- Phillips M.M., 1993, *ApJ*, 413, L105
- Piersanti L., Tornambé A., Straniero O., Domínguez I., 2009, in Antonelli L.A., Brocato E., Limongi M., Menci N., Raimondo G., Tornambé A., eds, *AIP Conf. Proc.* 1111. *Probing Stellar Populations Out to the Distant Universe*. Am. Inst. Phys., New York, p.259
- Pinsonneault M.H., Stanek K.Z., 2006, *ApJ*, 639, L67
- Pritchett C.J., Howell D.A., Sullivan M., 2006, *ApJ*, 683, L25
- Riess A.G. et al., 1998, *AJ*, 116, 1009
- Renzini A., 2004, in Mulchaey J.S., Dressler A., Oemler A., eds. *Clusters of Galaxies: Probes of Cosmological Structure and Galaxy Evolution*. Cambridge Univ. Press, Cambridge, p. 260
- Renzini A., 2006, *ARA&A*, 44, 141
- Ruiter A.J., Belczynski K., Fryer C., 2009, *ApJ*, 699, 2026
- Salaris M., García-Berro E., Hernandez M., Isern J., Saumon D., 2000, *ApJ*, 544, 1036

- Simon J.D. et al., 2009, *ApJ*, 702, 1157
- Sullivan M. et al. , 2005, in Turatto M., Benetti S., Zampieri L., Shea W., eds, ASP Conf. Series 342. 1604-2004: Supernovae as Cosmological Lighthouses. Astron. Soc. Pac., San Francisco, p.466.
- Sullivan M. et al. , 2006, *ApJ*, 648, 868
- Tammann G.A., 1977, *Mem. Soc. Astron. Ital.*, 49, 315
- Timmes F.X., Brown E.F., Truran J.W., 2003, *ApJ*, 590, L83
- Trimble V., 2008, *The Observatory*, 128, 286
- van den Heuvel E.P.J., Bhattacharya D., Nomoto K., Rappaport S., 1992, *A&A*, 262, 97
- Yamanaka M., et al., 2009, *ApJ*, 707, L118
- Yoon S.-C., Podsiadlowski Ph., Rosswog S., 2007, *MNRAS*, 380, 933
- Yungelson L.R., 2005, in Burderi L., Antonelli L.A., D'Antona F., Di Salvo T., Israel G.L., Piersanti L., Tornambé A., Straniero O., eds, AIP Conf. Proc. 797. Interacting Binaries: Accretion, Evolution and Outcomes. Am. Inst. Phys., New York, p.1
- Yungelson L.R., Livio M., 2000, *ApJ*, 528, 108
- Wang B., Meng X., Chen X., Han Z., 2009, *MNRAS*, 395, 847
- Webbink R.F., 1984, *ApJ*, 227, 355
- Williams K.A., Bolte M., Koester D., 2004, *ApJ*, 615, L49
- Woosley S.E., Weaver T.A., 1994, *ApJ*, 423, 371